UNIVERSIDADE D
COIMBRA

Shubhang Sharma

TRIBOLOGICAL BEHAVIOUR OF LASER TREATED C-ALLOYED TMD COATINGS IN RUBBER CONTACT

VOLUME 1

Dissertação no âmbito do Mestrado Conjunto Europeu em tribologia de Superfícies e interfaces orientada pelo Doutor Todor Vuchkov e o Professor Albano Cavaleiro e apresentada ao Departamento de Engenharia Mecânica da Faculdade de Ciências e Tecnologia da Universidade de Coimbra.

Julho de 2021

1 2 9 0

FACULDADE DE CIÊNCIAS E TECNOLOGIA
UNIVERSIDADE D COIMBRA

Tribological behaviour of laser-treated C-alloyed TMD coatings in rubber contact

Submitted in Partial Fulfilment of the Requirements for the Degree of European Joint European Master in Tribology of Surfaces and Interfaces.

Comportamento tribológico de revestimentos TMD ligados com C após tratamento laser para contatos com borracha

Author

Shubhang Sharma

Advisors

Professor Albano Cavaleiro

Doctor Todor Vuchkov

Jury

President	**Professor Bruno Trindade** **Professor at University of Coimbra**
Vowel	**Doctor Manuel Peralta Evaristo** **Investigator at University of Coimbra**
Advisor	**Doctor Todor Vuchkov** **Researcher at LED&MAT** **Instituto Pedro Nunes**

· U C ·

UNIVERSIDADE DE COIMBRA

tribos
Joint European Master in Tribology of Surfaces and Interfaces
Ljubljana • Leeds • Coimbra • Luleå

Coimbra, Julho de 2021

ACKNOWLEDGEMENTS

I would like to thank all the people who contributed in some way to the work described in this thesis.

First and foremost, I would like to express my gratitude to my advisor, Prof. Albano Cavaleiro and Dr. Todor Vuchkov, for their guidance in my research, their time, valuable comments and suggestions on this thesis. I am gratefully indebted to Dr. Todor Vuchkov without his intellectual and technical assistance, encouragement, and valuable suggestions on thesis writing, this thesis would not have been possible.

I would also like to thank TRIBOS consortium for providing me the opportunity of taking part in this program. I wish to acknowledge my TRIBOS mentors Prof. Ardian Morina, Prof. Mitjan Kalin, and Prof. Bruno Trindade for their support.

Finally, I must express my very profound gratitude to my family and to my batchmates especially Oday Allan for providing me unfailing support throughout my stressful times and through the process of researching and writing this thesis.

Abstract

Transition metal dichalcogenides (TMDs) in their hexagonal crystal structure offer very low friction and are used as solid, self-lubricating coatings. Pure TMD coatings are soft because of their open morphology and are usually doped with carbon to combine low friction with good hardness. Alloying of W-S films with C using sputtering techniques can result in an amorphous structure and decline the self-lubricious property in comparison with the pure WS_2 film, especially during sliding against rubber. The present study aims to improve the self-lubricity of a W-S-C coating using a laser treatment method. In fact, the influence of laser treatment was investigated by comparing the tribological behaviour among uncoated steel, pure WS_2, and untreated and treated WSC (50% at. C) coating. The chemical composition, morphology, and structure of the coatings were investigated using SEM/WDS, XRD, and Raman spectroscopy whereas hardness was evaluated by nano-indentation. To understand the tribological behaviour, a unidirectional pin on disc tribometer was used at room temperature. The wear tracks were investigated under a 3-D profilometer and SEM/EDS. Main conclusion was that the treatment using low laser power can cause WS_2 crystallization in the W-S-C coatings and, consequently, can improve their tribological properties.

Keywords Transitional metal dichalcogenides, Self-lubricating coating, laser treatment, Rubber tribology.

Resumo

Os dicalcogenetos de metais de transição (TMDs) com uma estrutura hexagonal oferecem atritos muito baixos e são usados como revestimentos sólidos auto-lubrificantes. Os revestimentos de TMD puro são macios devido às suas morfologias muito abertas e são usualmente ligados com carbono para combinar uma boa dureza com um baixo coeficiente de atrito. A adição de carbono usando técnicas de pulverização catódica dá origem a uma estrutura amorfa tornando difícil o caracter auto-lubrificante, em comparação com o WS_2 puro, especialmente durante o contato em deslizamento com borracha. O objetivo deste estudo é melhorar a auto-lubrificação de revestimentos do tipo W-S-C fazendo uso de tratamentos laser. A influência do tratamento laser foi investigada comparando o desempenho tribológico entre um aço não revestido e aços revestidos com WS_2 puro, e revestimentos W-S-C (50% at. de C) antes e após serem tratados com laser. A composição química, a morfologia e a estrutura foram analisadas por SEM/WDS, XRD, and espectroscopia Raman enquanto que a dureza foi avaliada por nanoindentação. Para compreender o comportamento tribológico, foi utilizado um tribómetro do tipo pino-disco e os testes foram realizados à temperatura ambiente. As pistas de desgaste foram analisadas com um perfilómetro 3D e observadas por SEM/EDS. A principal conclusão deste estudo foi que o tratamento com uma baixa potência de laser provocou a cristalização do WS_2 a partir do revestimento W-S-C e, consequentemente, permitiu melhorar as propriedades tribológicas.

Palavras-chave: Dicalcogenetos de metais de transição, Auto-lubrificação, Tratamento laser, Tribologia da borracha.

CONTENTS

1. INTRODUCTION

Reducing wear and friction in a system has always been a challenging task in order to design efficient yet reliable systems. In a passenger car, 28% of the fuel energy is dissipated in the form of friction that cost 208,000 million liters of fuel (gasoline and diesel) in 2009 to overcome friction in passenger cars worldwide [1]. Wear and friction can be overcome in various ways, for example, by low frictional coatings, topography and texturing, lubrication, etc. Lubrication not only reduces the friction but also plays a crucial role in increasing the efficiency and life cycle of any equipment. According to a study done by SKF, more than 50% of bearing failures are the cause of improper lubrication. The science that deals with the study of wear, friction, and lubrication at the interface of two contacting surfaces in relative motion is termed as tribology [2]. Liquid lubrication not only reduces friction between two contacting bodies but also lowers surface degradation, prevents damage, cleans the system, and provides cooling. But there are some systems where neither a liquid nor grease lubrication is suitable. In such problems, surfaces are coated to provide self-lubricity also known as solid lubrication.

The solid lubricants provide efficient boundary lubrication, reducing friction and wear under extreme operating conditions. Solid lubrication can be achieved by coating the material. Transition metal dichalcogenides (TMDs) have been one of the most widely used approaches to low friction coatings for tribological applications, particularly in dry and vacuum environments [3]. Thus, TMDs (Transition Metal Dichalcogenides) emerge as the focus of this research. On top of that, the properties of TMD coatings are enhanced by proper surface treatments. Furthermore, Laser treatment improves the tribological behavior of TMD coatings. Tribological behavior of TMD coatings highly depends on the operating condition such as temperature, humidity, loading, and most importantly the type of contact.

Solid lubrication is also used to solve various industrial problem e.g., polymer processing industry. Products produced during polymer moulding often get stick to the mould not only that but also deposits from previous items stick to the surface of the mould known as mould fouling and cause surface defects on the next product [4]. These problems limit the production rate of the process. Problems of mould release is a challenge yet not fairly studied and the problem remained less explored. The mould release agent can be introduced at the contact area that enables easy removal of the moulded part from the mould. Lubricity to the mould surface can be improved by applying chemical agents, however, this solution is not

permanent as the mould release agent in some cases has to be applied quite frequently. Sometimes in order to counter the problem during mould release process, it is also important to reduce adhesion between the mould and the moulding material. Adhesion can be reduced by reducing the surface energy of the mould surface which can can be achieved by coating the surface of the mould with a low surface energy material [5].

An effective way of correcting the situation is to use the low-friction adaptive coatings on the surface of moulds which facilitate the mould release process [6]. As the above problem can be interpreted as a metallic surface in rubber contact that is also the motivation behind studying the tribological behavior of TMD coatings using NBR rubber.

In this project, the tribological behavior of laser treated TMD coating in rubber contact is aimed to be investigated. TMD coatings will be deposited by using close-field unbalanced magnetron sputtering. Tribological testing will be performed by using a pin-on-disc tribometer. Various surface characterization techniques will then be used to understand the behavior of TMD coatings in rubber contact.

2. STATE OF THE ART

2.1. Tribology

The word tribology comes from the Greek word ’Tribos’ meaning ‘rubbing’ or ‘to rub’ and ‘ology’ meaning ‘the study of’. Tribology has undergone continuous evolution over time but came into the limelight from the so-called Jost report [2]. Science of tribology has been seen around since the very beginning of the stone age, 3500 BC [7].

Tribology involves the study of friction, wear, and lubrication between two interacting surfaces in relative motion [8]. This phenomenon can be observed in everyday life such as brakes in automobiles, cosmetics, and personal care products on our skin, and the consumption of foods such as chocolate, etc.

2.1.1. Friction

The parameter that quantifies the friction between surfaces is the coefficient of friction. It is defined as the ratio of the force opposing the motion to the normal force pressing the surfaces

together as shown in Figure 1.

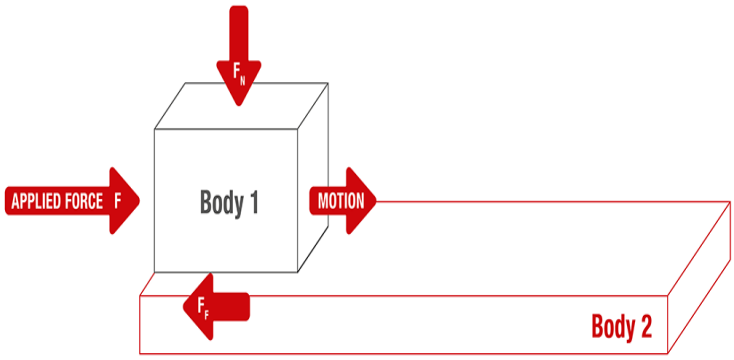

Figure 1 Schematic representation of friction of two bodies in relative motion [9]

Generally, friction has the following types:

Static friction: When two bodies in contact are about to move relatively, the force that opposes this motion is known as static friction. In other words, the static friction force must be overcome by an applied force before an object can move.

Kinetic Friction: The force that opposes the relative motion of two contacting bodies sliding over each other and rubbing together.

Rolling friction is observed when a body rolls on a surface, the force that opposes the motion of rolling is termed as rolling friction.

Fluid friction: This type of friction occurs when a solid object moves through a liquid or gas media, for example, when an aircraft is in flight.

Static, kinetic, and rolling friction corresponding to their coefficients of friction are denoted by μ_s, μ_k, and μ_r, respectively, and they usually follow the following order [9]:

$\mu s, > \mu k, > \mu r$

2.1.2. Wear

Wear is the removal of material from one or both of two solid surfaces in a solid-state contact [10]. Wear causes degradation of the functional surface in machinery that leads to loss of functionality. While determining the wear rate, various factors, such as the loading condition, temperature, and the nature of the motion between the contact surfaces is considered.

The distinction between friction and wear is that the former is the force acting between two

surfaces in relative motion, whereas wear is the phenomenon of mechanical and/or chemical damage that cause material degradation and poor surface properties. Common causes of machine failure are shown in Figure 2.

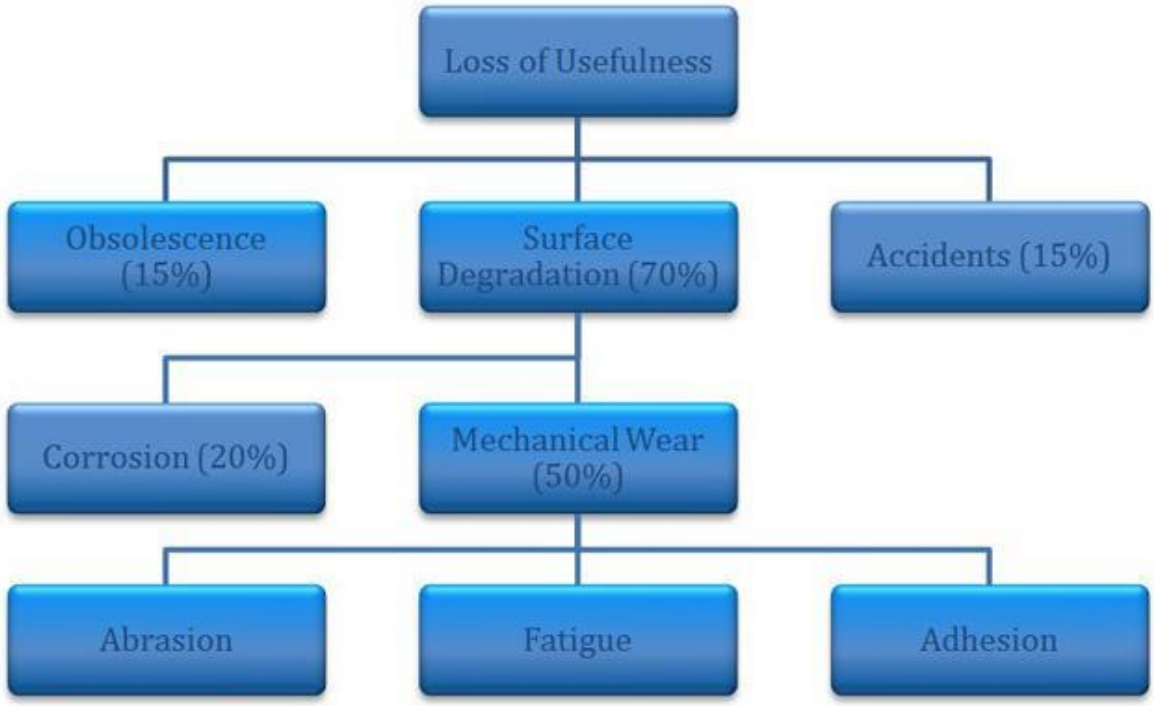

Figure 2 Common Causes of Machine Failures [11]

Wear can be classified as [11]:

- Abrasion causes abrasive wear that happens when a hard and rough surface of one object slides across the surface of another object that is significantly softer.
- Adhesive wear occurs when the displacement or attachment of unwanted substances or debris from one material adheres to the surface of another object.
- Fretting wear occurs as a result of repeated cyclical rubbing with a small amplitude of reciprocating motion between the surfaces of two different objects.
- Erosive wear occurs when solid or liquid particles of one material impinge against the surface of another.
- Surface fatigue is known as the weakening of surface material that occurs as a result of cyclic loading.
- Corrosion and/or oxidative wear that occurs as a result of chemical reactions between the worn material and a corroding medium.

2.1.3. Lubrication

Friction and wear can be controlled by inserting a lubricant between moving surfaces in contact. The lubricant used can be a fluid or a solid. Thus, lubrication not only increases the efficiency of the system by reducing the friction but also improves the life of machine equipment by preventing them from failures due to wear. Other roles of lubrication include cleaning of the system by getting rid of debris, cooling down the surfaces of contacting bodies, etc.

Oil and grease are the most commonly used lubricants. Grease is a mixture of oil and a thickening agent. Oils can be mineral-based, synthetic, or vegetable made as well as a combination of these. Vegetable oils are mostly environment friendly but in extreme conditions, synthetic oils are used.

The Role of a Lubricant [11]

The primary functions of a lubricant are to:

- Reduce friction
- Reduce wear degradation
- Protect the surface against corrosion
- Control temperature (dissipate heat)
- Control contamination and clean the equipment
- Transmit power (hydraulics)

The lubrication regime is defined by the lambda ratio (λ) [12]. The lambda ratio is the minimum film thickness (h_{min}) in relation to the composite surface roughness (R_{a_1} and R_{a_2}):

$$\lambda = \frac{h_{min}}{\sqrt{{R_{a_1}}^2 + {R_{a_2}}^2}}$$

The COF is inversely proportional to the pressure that is exerted on the contact surfaces and directly proportional to the difference in speed of the contact surfaces and the viscosity of the lubricant.

Figure 3 shows the Stribeck curve, which is the COF against $\mu w/p$ (speed (w), lubricant

viscosity (μ), and contact pressure (p)). There are three regimes as defined from the Stribeck diagram are given below:

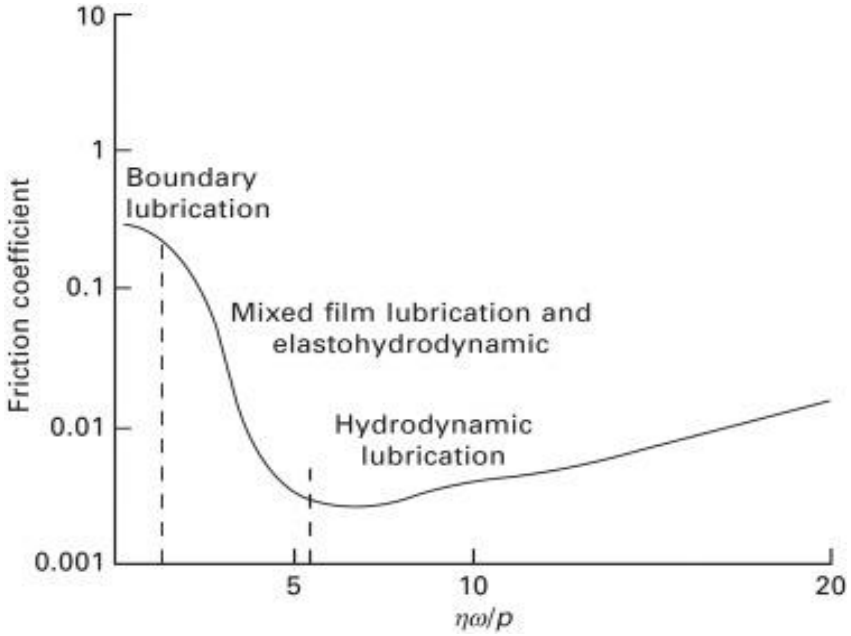

Figure 3 Stribeck Curve [12]

There are some systems where it is not feasible to apply oil or grease-based lubricants and also they can have detrimental effect on the contacting bodies. On the top of that, in some systems surfaces in contact are required of have self-lubricating abilities. To remedy these problems, researchers have been exploring the field of solid lubrication. Transition metal dichalcogenides (TMDs) are one of the most promising class of 2-D materials that can be exploited to achieve self-lubricating coating.

2.2. TMDs

Transition metal dichalcogenides popularly known as TMDs are the compound of Transition metals and chalcogen atom. Because of their unique crystal structure, TMDs offer very low friction and are used solid-lubricating coatings. There are commonly four different classes of solid lubricant materials: (1) carbon-based materials (e.g., graphite, DLCs, and nanocrystalline diamond); (2) TMD compounds (MoS_2 and WS_2); (3) polymers (PTFE); and (4) soft metals like Ag, Sn and Au [13].

2.2.1. Structure of TMDs

Transition metal dichalcogenide (TMDs) are generally represented by formula MX_2 where M is any transition metal and X is a chalcogen element. Transition metals (W, Mo, Nb) make covalent bond with chalcogens atoms (S, Se, Te) to form a mono layer. The phase of TMD

monolayers is entirely dependent on the electron count of transition metal in the d-orbital. The mono layers then make Van der waals bonds with adjacent layers to form multi layers.

The transition metal elements have what are known as d-electrons in their outermost electron shell which play an important role in determining the properties of TMDs. TMDs exist in two crystal form, hexagonal (2H-MX_2) and rhombohedral (3R-MX_2). TMDs are also found in disordered symmetry also known as turbostratic stacking. Structure of hexagonal TMD monolayer can be seen in Figure 4.

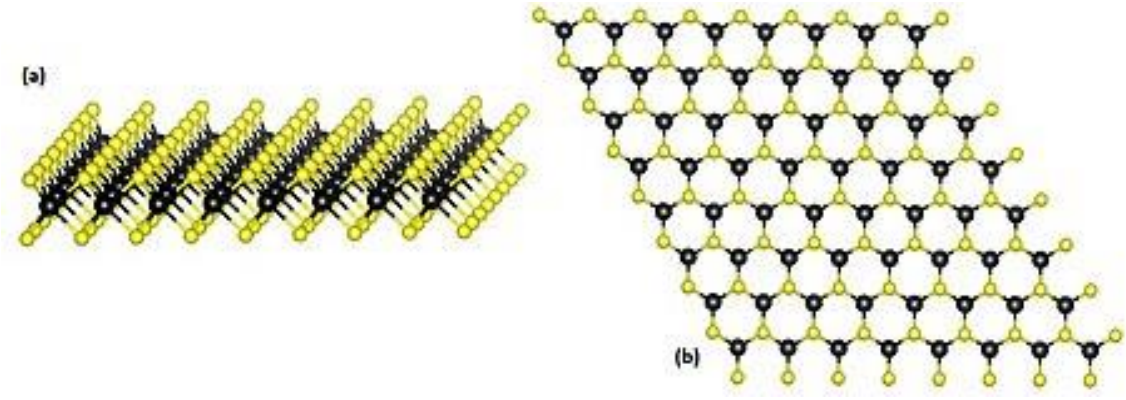

Figure 4 (a) Structure of a hexagonal TMD monolayer (M atoms are in black and X atoms are in yellow) (b) A hexagonal TMD monolayer as seen from above [14]

2.2.2. Properties of TMD coatings

Unlike graphene, TMD monolayer is three atoms thick, and each sheet consists of a layer of transition metal atoms such as molybdenum or tungsten between two planes of chalcogen atoms such as sulfur or selenium. Compared to graphene, 2D TMDs show high anisotropy and unique crystal structure [15]. Shear strength parallel to the planes is very low as a result when a normal load is applied to the surface of TMDs, adjacent layers slip on each other thus providing very low friction. Thus, there are three basic conditions require to have favorable tribological properties which are: 1) Minimal contaminations in TMDs as well as in surrounding e.g., H_2O creates problem in easy sliding of basal planes. 2) Adhesion between substrate and coating should be more than the force between lamellae themselves, resulting in preferential slipping between the adjacent layers and lowering the friction. 3) The reorientation of the basal planes in the tribolayer and the film favors in reduction of friction [16].

Voevodin et al. proposed for the first time to incorporate TMD lubricants into a carbon matrix reinforced with metal carbides to make such coatings that can provide low friction

and wear even in humid ambient air as well as in inert gas environments (dry N_2 and vacuum) [17]. TMD coatings are known to have super lubricity with a coefficient of friction around 0.001 against steel in vacuum environment [18]. Pure $MoSe_2$ coatings are soft with hardness below 1 GPa, whereas alloyed TMD coatings (e.g., C-alloyed TMDs) have a hardness ranging between 4 and 8 GPa [19]. Since the pure TMD coatings have columnar morphology and show poor adhesion, TMD coatings are alloyed with carbon to improve adhesion and hardness.

2.3. Nitrile rubber (NBR)

Nitrile Butadiene Rubber (NBR) is widely used as components of products where rubber-moving material is required due to its better tribological properties and resilience. Based on its properties, it is particularly used as oil and gasoline gaskets/seals, hoses liners, tubing, brake pads, O-rings, etc. C.L. Dongab conducted a sliding wear test under dry sliding conditions and analyzed the results related to ageing of NBR [20].

The aging has significantly altered the mechanical as well as tribological properties of the material. As aging and temperature were increased friction coefficient and shore hardness also increased. With the reduction in tensile strength and tear strength, the wear resistance of the rubber has significantly reduced. The wear mechanism was mainly due to the fatigue of rubbing pairs under dry conditions. However, aging and extreme service conditions are also a factor in material degradation and wear [21].

Under abrasive conditions, the NBR fluid sealing pairs exhibit certain behavior when subjected to sliding and abrasive wear tests [22]. The friction coefficient and wear rate changes which deteriorates the tribological performance. The friction coefficients are small for low abrasive concentrations but for higher abrasive concentrations, the friction coefficient increases. The seals were then attacked by hard particles, so the surface appears as pinned. As the particle concentration varies, the damage behavior varies. The high concentration of particles enters the rubber interface more easily. [22] Wear resistance losses more rapidly in the case of small size abrasive flow. The effect of aging NBR in hydraulic oil on the tribological properties is studied [21].

The NBR specimens were aged at high temperature for 70 days, and hardness, resilience, friction coefficient, and wear volume were analyzed. The friction coefficient was increased and had a detrimental effect on NBR material as seal ring degradation and failure.

Fillers and additives also affect the tribological properties of the material. For example, a

study conducted by Jian Yang indicates the addition of graphite powder fillers of different sizes affect NBR properties differently [23]. The more the graphite filler is added, the improved the tribological properties. The larger size particles provided a low friction coefficient to the matrix and the smallest particles give the best wear property.

2.4. Research gap

Deposition of MoS_2 usually leads to films with columnar structure with poor porosity and low hardness and the coatings deteriorate in the humid air [24]. Thus, their tribological behavior is unsuitable for high loads and moisture-containing atmospheres. Other transition metal dichalcogenides have similar properties to those of molybdenum disulfide, but some important drawbacks make them inappropriate for tribological applications. For example, it has been shown that pure niobium disulfides and diselenides exhibit poor lubrication properties due to their different electron structure concerning MoS_2 [25]. Common drawbacks of diselenides are low load-bearing capacity, low adhesion, and a detrimental effect of the moisture in the tribological contact, whereas the main drawback of sputtered tellurides is their strongly limited adhesion on steel substrates [26].

Tungsten disulfide (WS_2) is such a material which is used as a release material for plastic moulds, extrusion dies, and other release application [6]. Not only that WS_2 improves the service life of cutting tools and sliding parts, such as gearbox or bearings but also reduces excessive wear, seizing, and galling, as well as improves performance. Additionally, WS_2 is an inert and non-toxic material, therefore it has been used in medical device and food processing applications.

TMDs in their pure sputtered form are very soft because of the porous and columnar morphology that leads TMDs to have poor tribological properties like poor adhesion and low load-bearing capacity. Because of the poor performance of pure TMDs in moisture, TMDs are doped with metals like Ti [27], or non-metals like C [28]. These issues of pure TMD coatings can be solved by doping/combining with other elements that can either react with TMDs to form metal compounds or support them by forming nanocomposite coatings. Carbon is considered as one of the most promising elements for achieving stable nanocomposite low friction TMD coatings in diverse environments. But, it is worth noticing that doping with carbon leads to poor crystallinity resulting in a dramatic increment in the coefficient of friction. C-alloying costs loss in self-lubricity of the TMD coatings. In order to promote self-lubrication, either a high load is required or longer running-in time is needed.

Another way to promote self-lubricity is to trigger the formation of WS_2 crystals by partially treat the surface by laser [29].

Laser treatment is the surface treatment technique that can be utilized to improve the crystallinity and orientation of TMDs such as MoS_2 [29]. Laser treatment methods are mostly used to treat small volumes of the sample as a result overall mechanical property of the surface can be improved as the treated areas can act as reservoirs rich in more crystalline lubricious TMD phase. During sliding, the lubricious TMD phase originated from the treated zones can be smeared in the direction of sliding while the untreated areas can provide the load-bearing capacity.

However, the influence of laser treatment on mechanical properties and tribological behaviour of C-alloyed TMD coatings has not been studied much. Especially when alloyed TMD coatings are used in rubber contact e.g., during mould release, it is very difficult to promote self-lubricating behavior due to low load. Not many studies have been conducted to investigate the tribological performance of TMD coatings against rubber contact, more specifically NBR rubber.

2.5. Objectives of the research

Based on the aforementioned research gaps, this study aims to analyze and compare the tribological behavior of pure WS_2, carbon doped W-S-C, and laser-treated W-S-C coatings in relation to the application in the polymer processing industry. In fact, it is aimed to study whether laser treatment on surface of WSC coating induces the self-lubricating behaviour. The tribological behaviour of the above samples will be studied in rubber contact at room temperature. It is also aimed to evaluate hardness and investigate the coating using various characterization techniques. The main objectives and steps to achieve them are given below;

- Deposition of WS_2 and WSC (50 at. % C) by close field unbalanced magnetron sputtering.
- Partial surface laser treatment on WSC coatings using UV laser.
- Characterization of coating surface using SEM, WDS, XRD, and Raman Spectroscopy.
- Tribological testing using unidirectional pin on disc tribometer at room temperature.
- Analyzing wear tracks using SEM/EDS and 3 D profilometry.

3. METHODOLOGY

3.1. Material

AISI M2 steel is a molybdenum based high-speed steel in W-Mo series. HSS grade steel M2 is a medium alloyed high-speed steel that has good machinability. Its composition can be seen in Table 1.

Table 1 Chemical composition of AISI M2 Steel [30]

Material	*Fe*	*C*	*Cr*	*Mo*	*W*	*V*
M2 Steel	Balance	1%	0.4%	5%	6%	2%

Steel samples were ground using abrasive grit papers with grit size 240, 320, 400, 600, 800, 1200, and 2500. Mirror polishing was achieved with 6 μm and 3 μm diamond paste. A NBR rubber ball with a diameter of 10 mm was used as a counter-body.

3.2. Sample preparation

3.2.1. Physical vapour deposition (PVD)

High durability and strength are required for tools, engine parts and other parts used over a long period of time. Coating Technologies to enhance strength and durability include plating processes and various other techniques. Among these, physical vapor deposition or PVD has been used to deposit coatings with good adhesion and appropriate hardness in recent years. This technology has been frequently used for various applications. The technique allows growing a thin film at the atomic and molecular levels, with thicknesses ranging from several nanometers to several micrometers. It is possible to improve performance and properties in various ways, including reducing wear and enhancing heat resistance.

Generally, there are two types of PVD techniques for thin film deposition in vacuum conditions, evaporation, and sputtering techniques. In the process of evaporation, the raw material is heated and evaporated using a thermally heated filament or high-energy electron beam. Vacuum promotes transferring of vapored material to the substrate where it is condensed [31].

The other PVD technique is sputtering, and for the purpose of this document magnetron

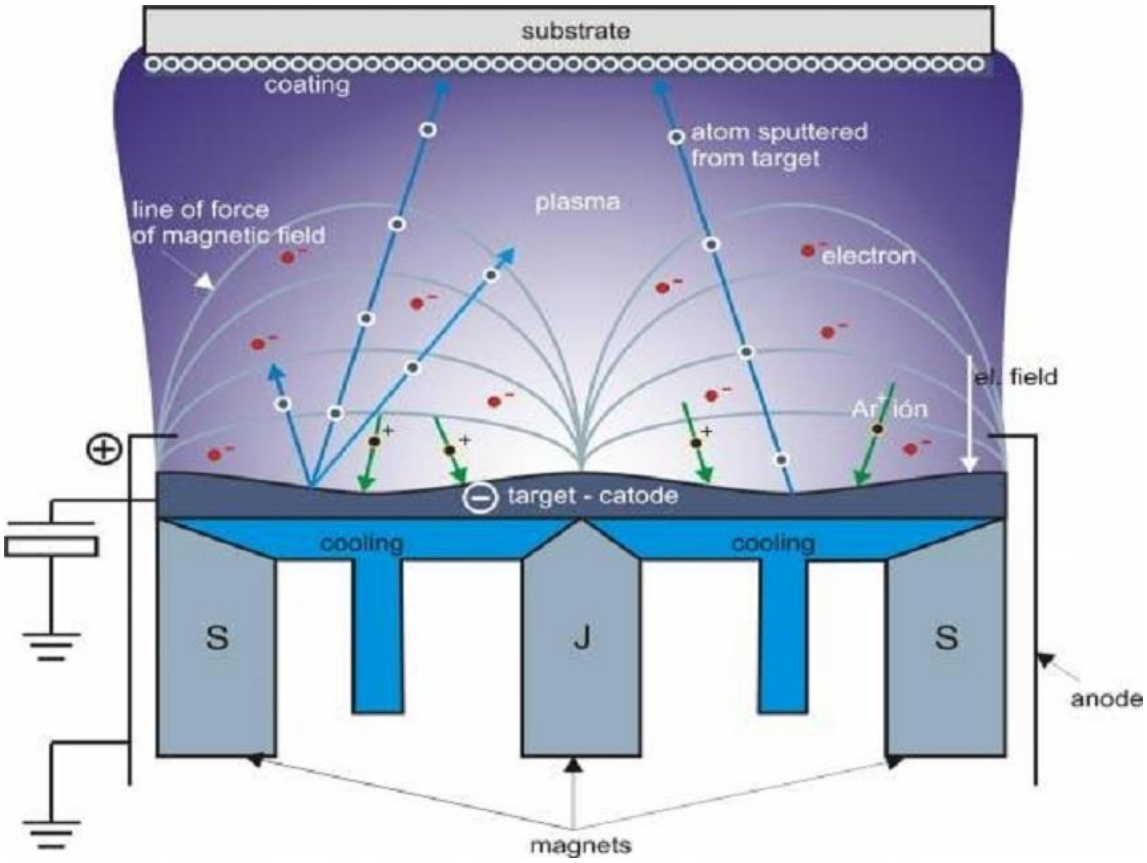

Figure 5 Magnetron sputtering technology [52]

sputtering will be explained more in detail in the next section since it has been used to prepare the thin films in this work.

3.2.2. Magnetron Sputtering

Sputter deposition simply called sputtering, is an entirely different process than the other types of thin-film deposition. In this process atoms or molecules of a material from a target are ejected by the bombardment of high-energy particles. Erosion of target material leads to the formation of a charged cloud that deposits on the substrates. There are various configurations of sputtering, including DC diode, RF diode, magnetron sputtering, etc. However, diode sputtering has some disadvantages, such as very low deposition rates and high cost. During magnetron sputtering process, a closed magnetic field parallel to the target surface is added to enhance the ionization efficiency as the secondary electron generated due to the bombardment of Ar ion with the target is bound to a specific area of the target surface by means of the orthogonal electromagnetic field formed on the surface of the target, resulting in the growth of ion density and energy, and finally realizing the high-rate sputtering. A schematic representation of the working principle of magnetron sputtering can be seen in Figure 5.

Some of the advantages of magnetron sputtering include [32] :

- High discharge currents, low voltage.
- Coating thickness up to about 5μm.
- Deposition rates range from 1 nm/min to 10 nm/min, excellent uniformity, pure and dense coatings, excellent coverage of steps and small features, ease of automation.

On the basis of the distribution of magnetic field configuration, magnetron cathode is classified as balance and unbalanced magnetron cathode. There were series of research performed to study the tribological behaviour of carbon alloyed TMD coatings. Influence of alloying with varied carbon percentage on tribological performance of TMD were studied under different conditions such as loading, contact geometry, and environment. The best results in those studies were obtained in case of W-S-C and Mo-Se-C coatings. The carbon content of W-S-C coatings with promising tribological performance was ~50 at. %. A low COF was reported for sliding in dry environments [24], [16], [33].
In this work, a closed field unbalanced magnetron sputtering process was used to deposit the WS_2 and WSC (50 at. % C).

3.2.3. Deposition procedure

Films were deposited on top of M2 steel and silicon wafers using UDP 650/4 Teer Coatings deposition equipment. Before placing the steel substrate (polished to a 3μm diamond finish, R_a < 20nm) on a rotating fixture in the chamber, the steel sample was ultrasonically cleaned for 15 minutes each in acetone and ethanol. The rotating fixture was placed at a target to substrate distance of ~ 25 cm. The deposition procedure was similar for both WS_2, and WSC coatings except for the usage of graphite targets.

To deposit WSC, two graphite, one WS_2, and one Cr targets were mounted on the magnetrons inside the chamber, and a pressure of < 5 x 10^{-4} Pa inside the chamber was achieved. The targets and the samples were sputter cleaned simultaneously in pairs for 20 minutes each pair to prevent cross-contamination.

The idea of depositing chromium interlayer is to improve adhesion between the WSC film and the steel substrate. The deposition of the Cr interlayer took 10 min and a thickness of ~200-300 nm was achieved. Power to the Cr target was reduced and power to WS_2 and graphite targets were increased to 1000 W and 1500 W (on each), respectively, which

resulted in W-S-C coating with ~50 at. % C.

3.2.4. Surface laser treatment

Laser surface treatment is effectively a thermal process that heats the surface by light adsorption. The adsorbed energy produces a thin layer on the surface with modified properties, leaving the bulk unaffected [34]. Surface laser treatments are a reliable technique for tailoring chemical, optical or electrical properties of TMDs. The surface treatment employed in thinning of layered TMDs as well as laser-induced site-specific doping. Electrical conductivity can also be enhanced by laser-assisted oxygen passivation of chalcogen vacancies. Tariq Afaneh at el., carried out and studied Laser treatment experiment for WSe_2 or $MoSe_2$ TMDs in H_2S environment [35]. The laser-assisted surface treatment was done on ultrathin TMDs, in which the Selenium atoms were replaced by sulfur atoms from the gas environment. The irradiation imparts changes in creating Selenium vacancies via local heating while dissociating the environment gas i.e. H_2S. After evaluating the results in the study by Tariq Afaneh at el., it was found that the laser wavelength of 532nm produced better results as compared to longer wavelengths of 632nm [35] as high laser power irreversibly damages the crystal structure. Alternatively, low laser power does not significantly affect the Selenium atoms or created chalcogen vacancy for chemical exchange. Optimized laser power, laser exposure time, and gas environment are the crucial parameters to have controlled composition and crystalline quality of the TMD films.

For the purpose of the work performed in this document, laser surface treatment is the subject of interest from laser processing technology. Surface treatment via laser technology is performed to improve surface-oriented properties such as hardness, fatigue strength, wear resistance, and corrosion resistance [36].Surface melting, surface hardening, and structural transformation are a few examples of the desired effects of laser surface treatment. Due to its capability and high precision control, the technique possesses a significant presence in thin-film treatment.

Laser surface treatment is a proven technique to transform TMD film from amorphous structure to crystalline structure. TMD films that are deposited by sputtering at low temperatures (less than 250 °C) will have low crystallinity or even amorphous structure [37]. However, crystallization of TMD films such as MoS_2 and WS_2 via laser treatment has been reported with relative success [37], [38]. Laser-induced phase transformation of TMD is especially valuable for friction-reducing applications as it allows transformation at very

precise regions on the surface.

Nd:YAG Laser is a type of solid-state laser that uses crystal yttrium aluminium garnet (with chemical formula $Y_3Al_5O_{12}$) host with neodymium impurities. Nd:YAG lasers have wavelength of 1064 nanometers, which belongs to the near-infrared region. At its wavelength, Nd:YAG lasers offer higher absorption for most engineering materials compared to other laser types [39]. Another important advantage of Nd:YAG laser is its small spot size which allows for higher process efficiency. Due to its inherent advantages, Nd:YAG laser is prevalent in numerous fields.

The type of laser that will be used in this work is the ultraviolet laser. Ultraviolet lasers are usually produced by an excimer laser. Though gas lasers can also produce ultraviolet light, they do not have the efficiency and the access to power compared to excimers [40]. Ultraviolet light has shorter wavelength compared to infrared or visible light; hence it carries greater energy. It is clear then that most of the advantages of ultraviolet laser are due to its superior photon energy. In fact, ultraviolet lasers find applications in chemical or biological research because the energy of its photon is larger than the binding energy of numerous molecules [40]. This detail also makes ultraviolet lasers attractive for surface treatment applications. Since ultraviolet photons carry enough energy to directly break the binding energy of molecules, laser treatment using ultraviolet lasers is described as a “cold process”. This results in minimization of the heat-affected zone on the surface, allowing for surface modification with greater precision.

In this work a diode-pumped pulsed UV (355 nm) Inngu Laser, with maximum power of 3 W fitted with a scan head with a F-theta lens (160 mm focal distance, 100 × 100 mm^2 max. scanned area) was used to apply dot pattern laser treatment on the W-S-C coatings. The spacing between the dots was set to be regular and the programmed sketch was an uniform square grid of dots (pulse center) separated by 20 μm. The laser treated samples were provided by the Physics department-University of Aveiro.

3.3. Surface Characterization Techniques

3.3.1. Scanning electron microscope

When the electrons interact with the sample, it results in various kinds of interaction. The information that is carried by each type of interaction is collected by different kinds of detectors. Electron-sample interaction is shown in the given Figure 6.

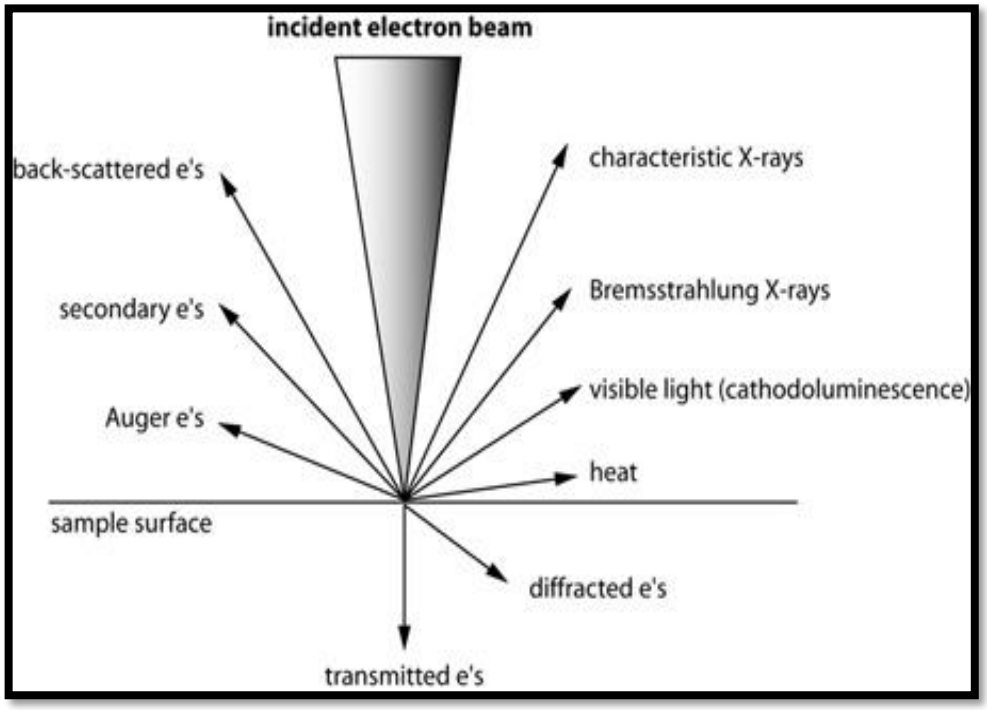

Figure 6 Electron-Sample interaction adapted from [41]

The scanning electron microscope uses a highly focused beam to interact with the sample. The kinetic energy of electrons is dissipated in the form of a variety of signals. The voltage applied to accelerate electrons in SEM is typically in a range of from a few to 30 keV [42]. Generally, secondary electrons, backscattered electrons, and X-ray diffraction are the main focus of using SEM. Secondary electrons allow investigating morphology and topography, whereas backscattered electrons help in illustrating the contrasts in composition in samples having multiple phases. X-ray diffraction enables us to investigate chemical composition using energy dispersive spectroscopy or wavelength dispersive spectroscopy. The SEM images have very high resolution (up to 10 [nm]) and a large depth of field [43].

A field emission SEM (Zeiss Merlin) was used to investigate the surface morphology of the coating. The chemical composition was performed using WDS equipment mounted on the SEM. Oxford X-Max 20 Silicon Drift Detector with a detector size of 20 mm^2 was used for energy dispersive spectroscopy (EDS) analysis.

3.3.2. Raman spectroscopy

Raman spectroscopy is an optical, vibrational spectroscopic technique which is used to provide molecular composition and molecular structure [44].

The Raman Spectra gives the molecular fingerprint, and it is different for different molecules. Thus, Raman spectroscopy for a particular molecule helps in performing qualitative analysis, similarly, the intensity of a particular Raman line helps in determining the concentration of the molecule in a sample, this manner, quantitative analysis can be done. Thus, Raman spectroscopy can be used to perform both qualitative and quantitative analysis of the sample.

The micro-Raman analysis was conducted in the backscattering configuration on a Horiba HR800 instrument using a 600 lines mm^{-1} grating and the 441.6 nm laser line from a HeCd laser (Kimmon IK Series, Japan).

3.3.3. XRD

X-ray powder diffraction (XRD) is used for phase identification of a crystalline material and can provide information on unit cell dimensions [45]. X- rays undergo diffraction when passes through a crystal since the X-ray wavelengths (between 0.2 and 10 nm) are comparable to the interatomic spacing of crystalline solids [46]. XRD's principle is based on the Bragg's law:

$$n\lambda_x = 2d\sin\theta$$

- λ_x-wavelength of the X-ray,
- d-spacing between the crystal layers,
- θ-incident angle, and
- n is an integer.

The XRD analysis in this work was carried out on Phillips equipment, using grazing incidence configuration. This instrument uses the Co Kα radiation for X-rays. The scanning angle range was 5-90º (2θ).

3.3.4. Nanoindentation

Nanoindentation is a technique used to measure the hardness of a material. Nanoindentation is a powerful quantitative method for obtaining mechanical properties from

very small volumes [47].

The working principle of the nanoindentation technique is based on the plastic deformation of materials under a load. An indenter (Berkovich diamond pyramid indenter) is used to determine the hardness and Youngs modulus of the coatings. Hardness, H, is the ratio of the maximum load, F_{max}, during the indentation to the contact area of the indentation, A_c, immediately before unloading.

$$H = \frac{F_{max}}{A_c}$$

The NanoTest (Micro-Materials Ltd.) nanoindentation equipment was employed to measure hardness and young's modulus of the samples using a Berkovich diamond pyramid indenter. A map was made using 7x7 indentation with 5 microns distance between them. A maximum load of 3 mN was set which resulted in indentations within the coatings.

3.3.5. 3-D profilometer

Generally, there are at least two parts of a profilometer – a detector and a sample stage. The detector determines the points on the sample and the sample stage is to hold the sample.

Normal light-sensitive cameras can capture the image from an optical microscope to generate a micrograph. Originally images were captured by the photographic film but modern developments to the charge-coupled device, CCD cameras, allow the capture of digital images. Purely digital microscopes are now available what uses a CCD camera which examines a sample and shows the resulting image directly on a computer without the need for eyepieces. For this work a 3D white light interferometer was used (Rtec Instruments).

3.4. Tribological Testing

Pin on Disc tribometers are probably the most known and extensively used devices in tribology. In this type of configuration, the tribometer consists of a rotating disc and a stationary pin as shown in the Figure 7. Controlled systems are used to apply constant loading on the stationary pin. A pin can have different shapes, flat, triangular, or spherical.

The Reciprocating Sliding wear tester can be used to measure average COF and wear rate. Wear tracks can be studied separately under microscopes. It is possible to perform both dry and lubricated tests. Different types of contact geometries are possible such as pin-on-plate or pin-on-disc [48]. Load, frequency, stroke length, and temperature can be varied using controlled systems according to requirements.

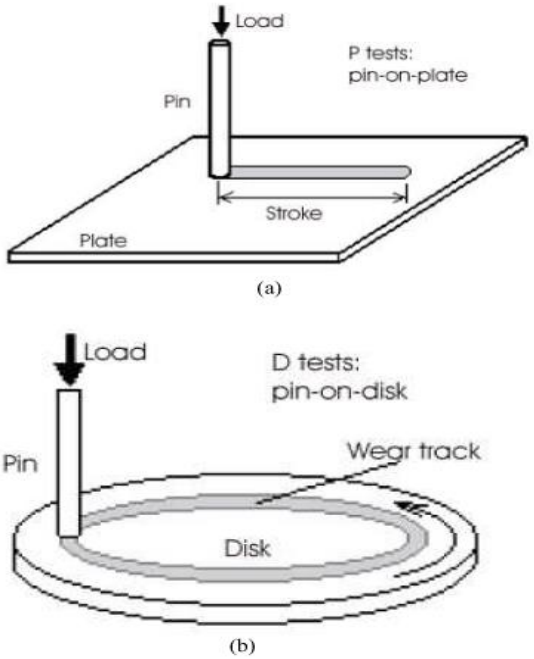

Figure 7 Geometric representation of a) Reciprocatory b) Sliding wear test in pin on disc configuration [48]

A tribological test will be performed using a unidirectional pin on disk device (RTEC instrument). Testing conditions are given in Table 2.

Table 2 Pin on disc test conditions

Testing conditions	
NBR Ball	10mm
Normal load	10 N
Sliding speed	0.05 m/s
Temperature	25°C
Cycles	5000
Radius of sliding circle	10mm

4. RESULTS AND ANALYSIS

This project is aimed to study the effect of partial laser treatment on the tribological behaviour| of WSC coating alloyed with 50% at. C in rubber contact. In fact, this study compares the tribological and mechanical properties of M2 steel, Pure WS_2, untreated WSC50, and laser-treated WSC50. Morphology and structural characterization of the coating were investigated as well as hardness was evaluated. Finally, frictional behaviour and wear analysis were conducted to understand the tribological behaviour of TMD coatings in rubber contact.

4.1. Chemical composition and morphology

Elemental chemical composition was investigated using WDS analysis as shown in Table 3. As expected, the S/W ratio was decreased in the case of WSC coatings. The carbon concentration in WS_2 coating is most likely due impurity of the target due to the contamination during manufacturing or usage during the deposition of coatings containing carbon. The presence of oxygen is typical in the case of films deposited by co-sputtering. The decrease of O percentage in WSC coatings compared to WS_2 coatings can be due to the chemical reactions taking place inside the chamber during the process of sputtering. In the discharge atmosphere, active C species are present, leading to the bond formation with O atoms to form CO or CO2 gas, which are then pumped out from the chamber. Another factor attributed to the decrease of O in these films is the reduction of specific area exposed to the environment due to improved coating density due to carbon alloying [33].

Table 3 Elemental chemical composition

	Elements (%)				
	W	S	C	O	S/W ratio
WS_2	34	55.5	4.1	4.8	1.63
WSC	20.3	28.7	48	2.6	1.41

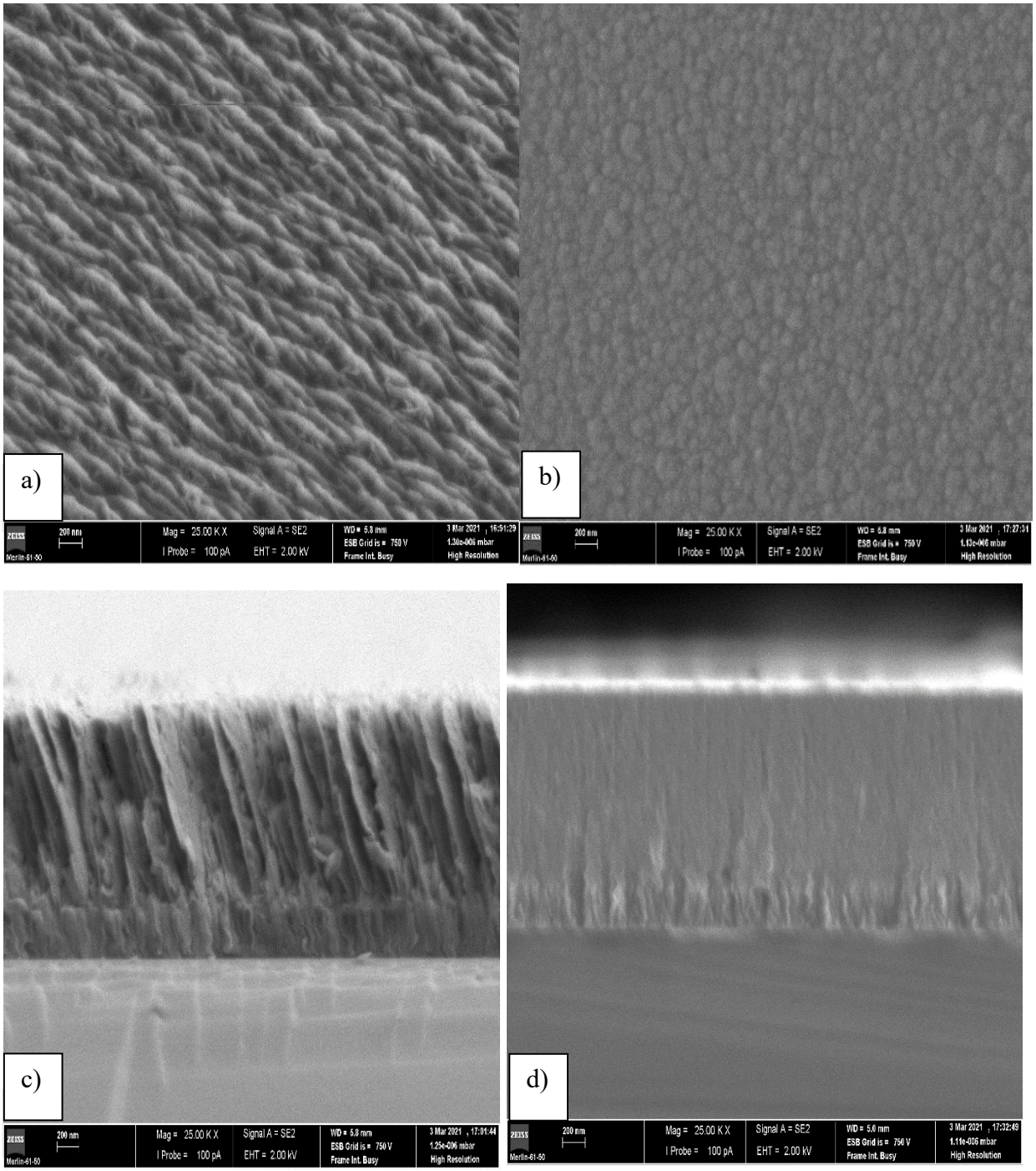

Figure 8 Images under SEM a) WS_2 (top view) b) WSC (Top view) c) WS_2 (cross-section) b) WSC (cross-section)

WS_2 and WSC (50% at. C) coatings were investigated under a Scanning Electron microscope. Both Figure 8 a and b show a porous and cauliflower-like morphology which is typical for TMD films deposited by the PVD process [28].On the other hand, the morphology in the case of WSC appears to be denser and smoother. Figure 8 c shows a columnar structure that is inherently porous, whereas Figure 8 d shows denser compact morphology as expected [28]. The coating thickness is found to be ~1.5 1.425 μm for both coatings, whereas the interlayer is ~0.2-0.3 μm thick.

4.2. Structure

From the XRD diffractogram, as shown in Figure 9, it can be observed in the case of pure WS_2 coating that there was a peak observed at $2\theta \approx 14°$, indicating the plane (002) parallel to the substrate corresponds to 2H-WS_2 phase as reported by Regula et al. [49]. The other two asymmetrical peaks indexed as (100) and (103) at $2\theta \approx 38°$ and $2\theta \approx 46°$ respectively (ICDD Ref No 01-084-1398).

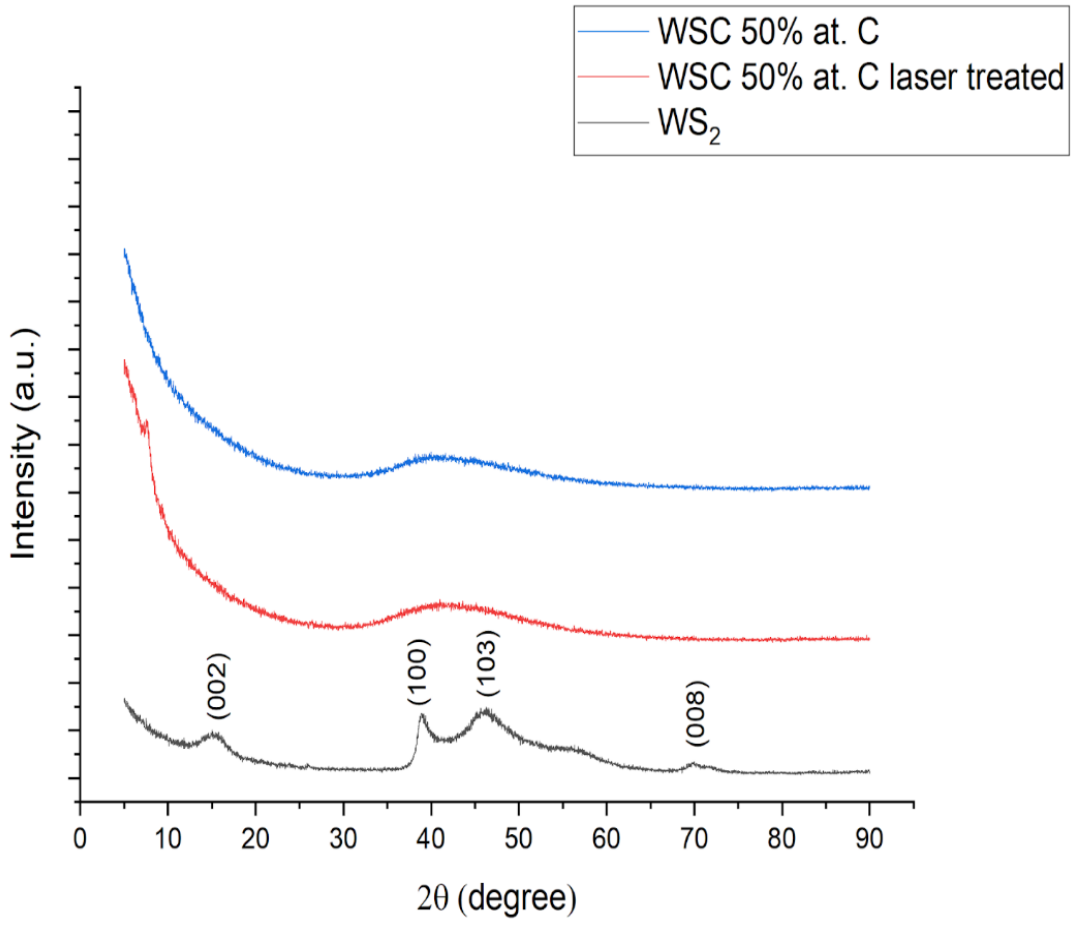

Figure 9 XRD diffractogram of deposited coatings

Plane (100) signifies that some of WS_2 crystals are oriented perpendicular to the substrate. With the presence of an increasing C content for the alloyed coatings, these peaks become broader with decreasing crystalline domain size. For these films, only one very broad peak is observed at the same positions ($2\theta \approx 30° - 50°$) of the (10L) line of the WS_2 phase. However, there is not any distinct and intense peak in diffractograms of UV-laser-treated samples. The XRD technique could not observe the crystallization of WS_2, very likely due to the small size of the crystals.

Raman spectroscopy which is an efficient method to understand the chemical identification

and the structural analysis of WS_2 and carbon was performed on WS_2 and WSC coatings. Table 4 shows band positions of 2H-WS_2 single crystals, D and G bands of carbon [50].

Previous literature has shown that there are three zone-center Raman active modes in monolayer 2H-TMDs which are represented as A1g, E1g, and E2g [50]. Two of them (A1g and E1g) are usually observed in the backscattering configuration, in which the presented results have been obtained. In our experiments, the corresponding A1g and E1g Raman scattering peaks in case of WS_2 were obtained at 418 cm^{-1} and 357 cm^{-1}, respectively as shown in Figure 10. It is widely accepted that the broadening of the latter line results from a double 2LA(M) process, whose peak emerges at 352 cm^{-1} in the spectrum.

Table 4 The band position of WS_2 and carbon

Category	Band	Wavelength (cm^{-1})
2H- WS_2	A1g	418
	E1g	357
	LA (M)	352
Carbon	G	1560
	D	1385

In case of WSC50, peaks related to WS_2 crystals were absent indicating loss in crystallinity. However, two modes of carbon band were observed namely D mode and G mode. When nanocrystalline graphite changes into amorphous carbon, G peak moves from 1600 cm^{-1} toward lesser Raman (1560 cm^{-1}), and the I(D)/I(G) ratio decreases; Increasing dispersion of the G peak. Thus, this kind of shift and dispersion in peak's position indicates manifestation of amorphous structure [50].

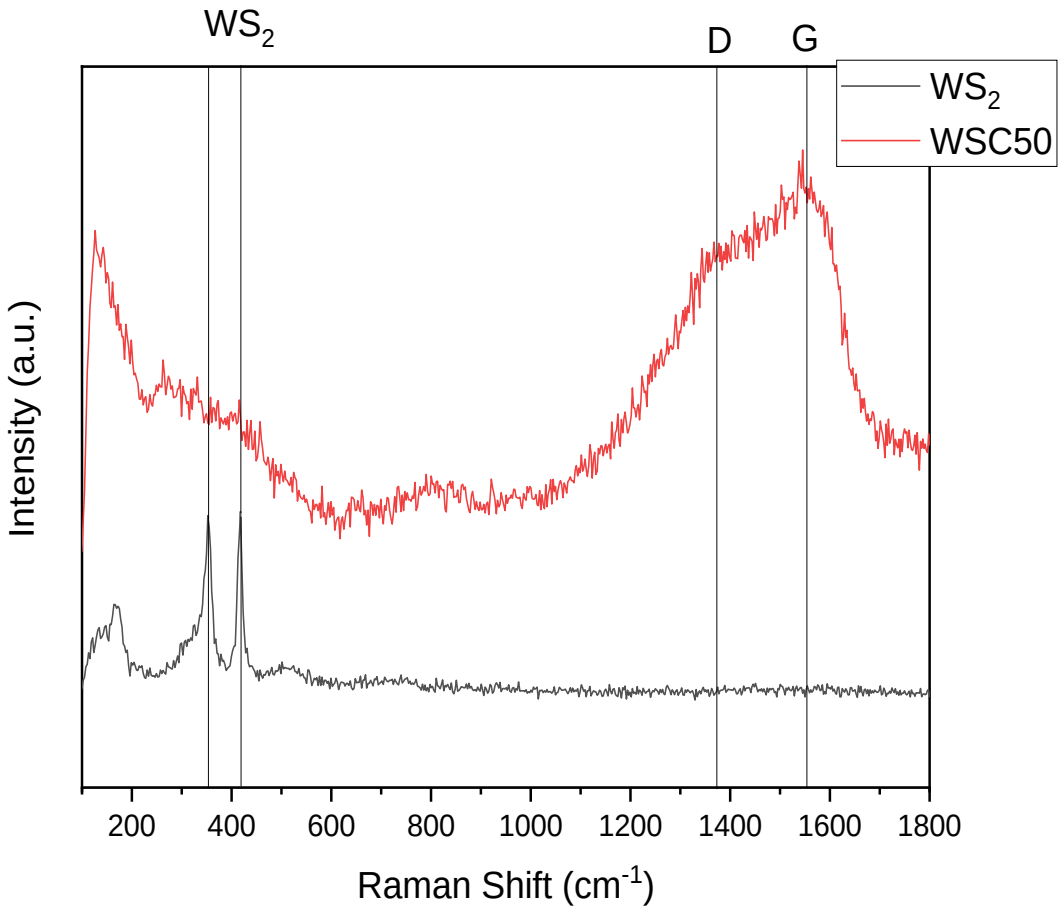

Figure 10 Raman spectra of WS_2 and WSC coatings

Figure 11 shows an optical microscopic picture of UV laser-treated WSC50 sample, and Figure 12 shows Raman spectra of three different points on the surface. Peaks corresponding to WS2 at wave number 356 and 421 cm^{-1} clearly show increased crystallinity after laser treatment. Other peaks at 1385 and 1560 cm^{-1} which are D and G bands of carbon, were also observed. Appearance of peaks 356 and 421 cm^{-1} justifies the crystallization of WS2 in the structure which might result in better tribological performance. On the other hand, moving of G peak from 1581 to 1600 cm^{-1} and increasing of I(D)/I(G) ratio would prove the graphitization of the structure [70]. According to Figure 13, both Point 22 and Point 42, which are brighter than Point 21, demonstrate WS_2 peak and D peak shoulder at around 1385 cm^{-1}. By comparing peaks position of point 21 and untreated WSC50 Raman spectra, it can be observed that the I(D)/I(G) ratio has increased meanwhile G peak has shifted to 1600 cm^{-1}, which means an increase of sp2 content in the film associated with the progress of graphitization.

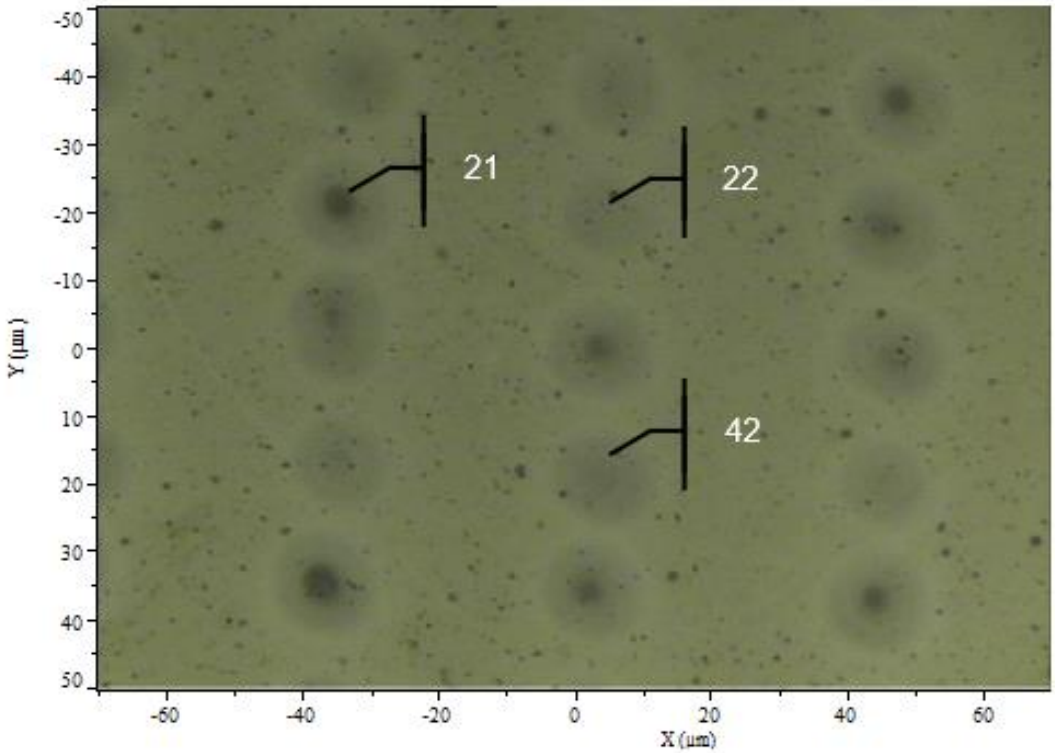

Figure 11 Optical microscope picture of laser-treated WSC50

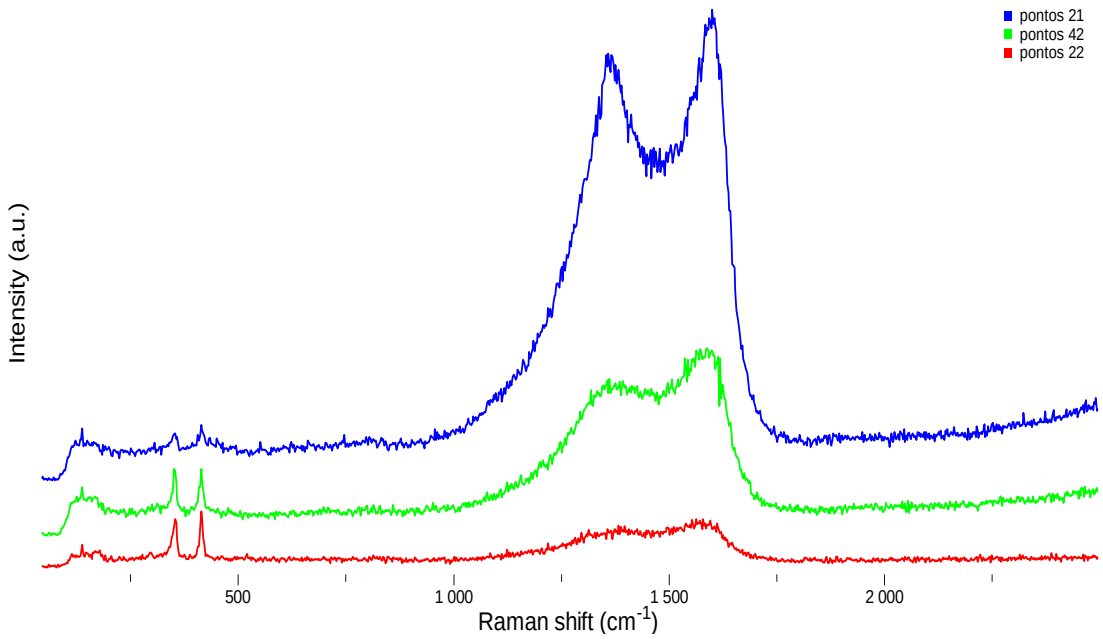

Figure 12 Raman spectra at 3 different points for laser treated WSC50

4.3. Hardness

The hardness of coatings was found by the nanoindentation test. In the treated area, the hardness was down to 2.9 GPa whereas overall hardness was down to 5.6 GPa. In fig. 8, the graphs between load and indentation depth are shown and it was found that reduced young's modulus was also decreased after laser treatment. Figure 13 shows the response of coating surface to load vs indent depth.

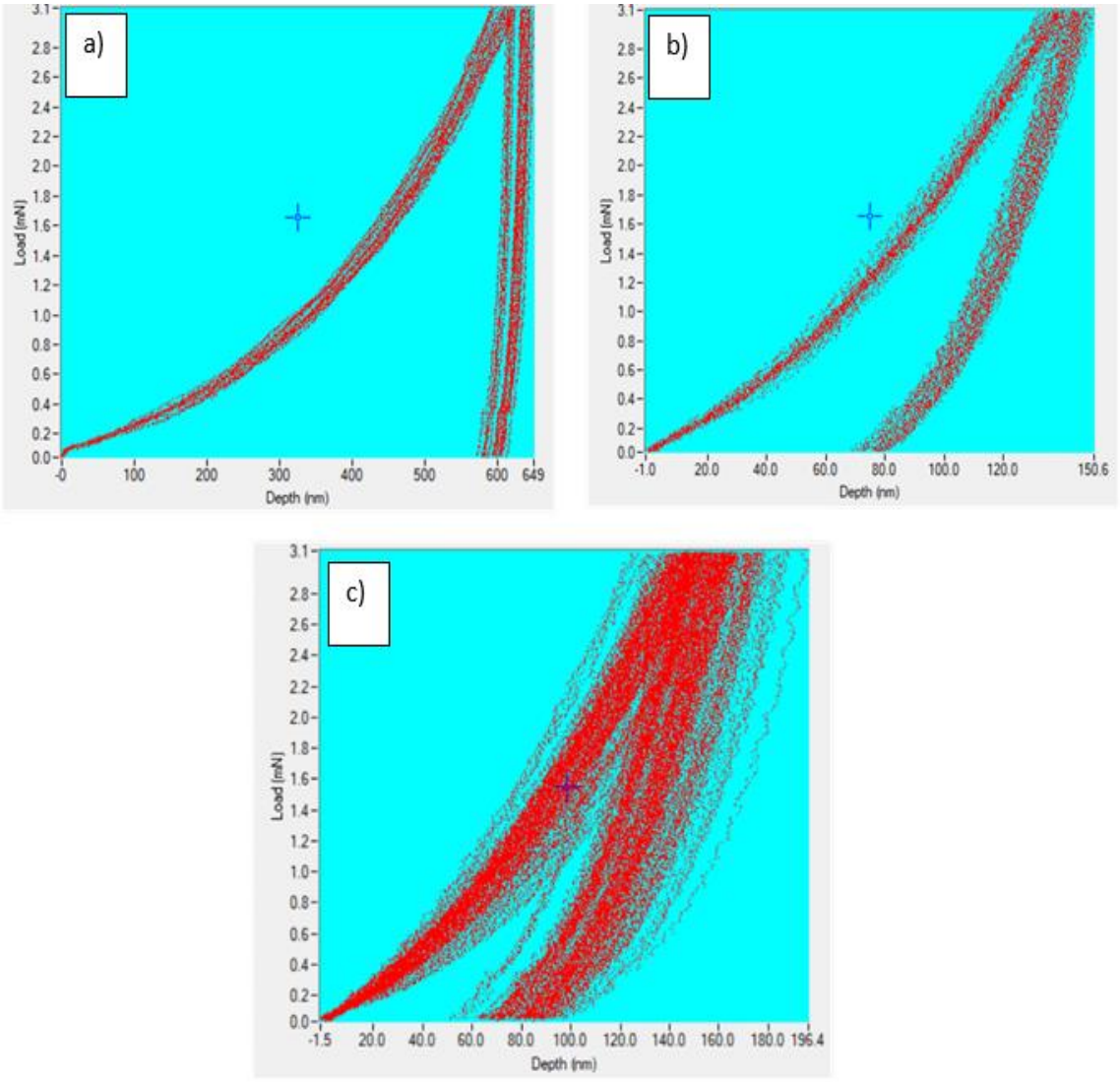

Figure 13 Load vs indentation depth a) WS2 b) WSC50 c) WSC50 laser-treated

The hardness values measured in W–S–C films are similar to those obtained by Voevodin et al. [17]. WSC50 coatings were harder, 6.3 GPa as compared to pure WS_2 coatings, 0.32 GPa as shown in Figure 14. It is because WS_2 films are soft due to their columnar and porous morphology, whereas alloying with carbon results in the compact and dense coating, making

them harder. As a result, alloying of TMD coatings with carbon results in an increase in load-bearing capacity.

In case of laser-treated WSC50 coatings, more than 70% of its surface has been treated and due to over exposure by laser, the irradiated area has been either graphitized or oxidized.

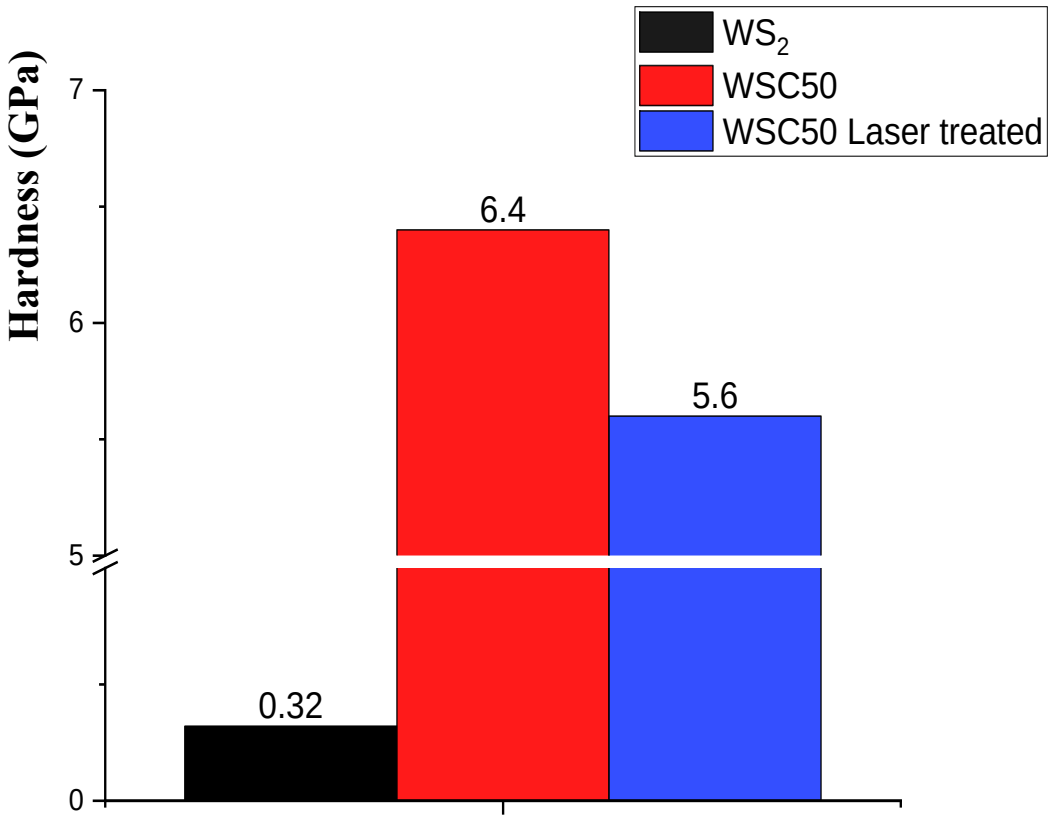

Figure 14 Hardness comparison of WS2, WSC50 and laser treated WSC50

The low value of hardness in the free surface, also could be related to the closeness of this area to irradiated spots.

4.4. Tribological behaviour

The frictional behaviour of TMD coatings depends on various factors like the nature of the material, contact geometry, environment, load, and so on. In this project, parameters such as sliding speed, temperature, number of cycles, and load were kept the same for all the samples.

4.4.1. Frictional behaviour

The sliding process undergoes two different stages namely running in and steady-state. Except in the case of WS_2, other samples could not reach the steady-state stage as the number

of cycles was not enough, although it is also likely that dry sliding against rubber can result in unstable COF due to continuous degradation of the rubber counterpart. The most stable and lowest COF was observed in the case of WS_2 coatings i.e., $\mu \sim 0.34$ and uncoated steel showed the highest value i.e., $\mu \sim 1.3$. Here COF is the average value during the entire test. Laser treated WSC coating appeared to have a slightly lower average COF (~1.2) as compared to untreated WSC ($\mu > 1.13$). The comparison of COF is shown in the Figure 15.

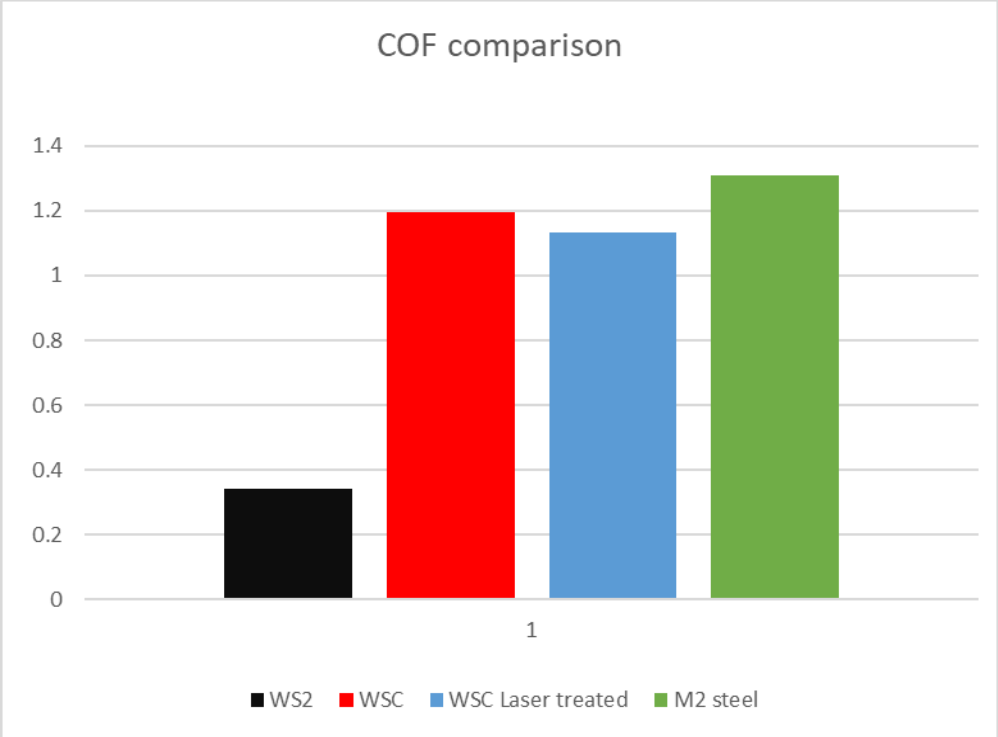

Figure 15 Comparison of average COF for all the four samples

In comparison to untreated WSC50 coating, WSC50 laser-treated coating showed reduced COF up to 2200 laps but after that COF increased and became almost the same as untreated WSC50. Comparison of average coefficient of friction among the samples shows that laser treatment was able to reduce COF but as the running in time passes, the lubricious surface is removed and WSC50 laser-treated coating starts to behave like untreated WSC50 coating. The trend observed at room temperature is shown in Figure 16.

Untreated WSC coating showed a reduction in coefficient of friction after aproximately 500 laps which can be explained due to the reorientation of basal planes due to sliding and, after around 3000 laps, COF increased dramatically most likely due to degradation of NBR rubber as reported by Geet et al. [51].

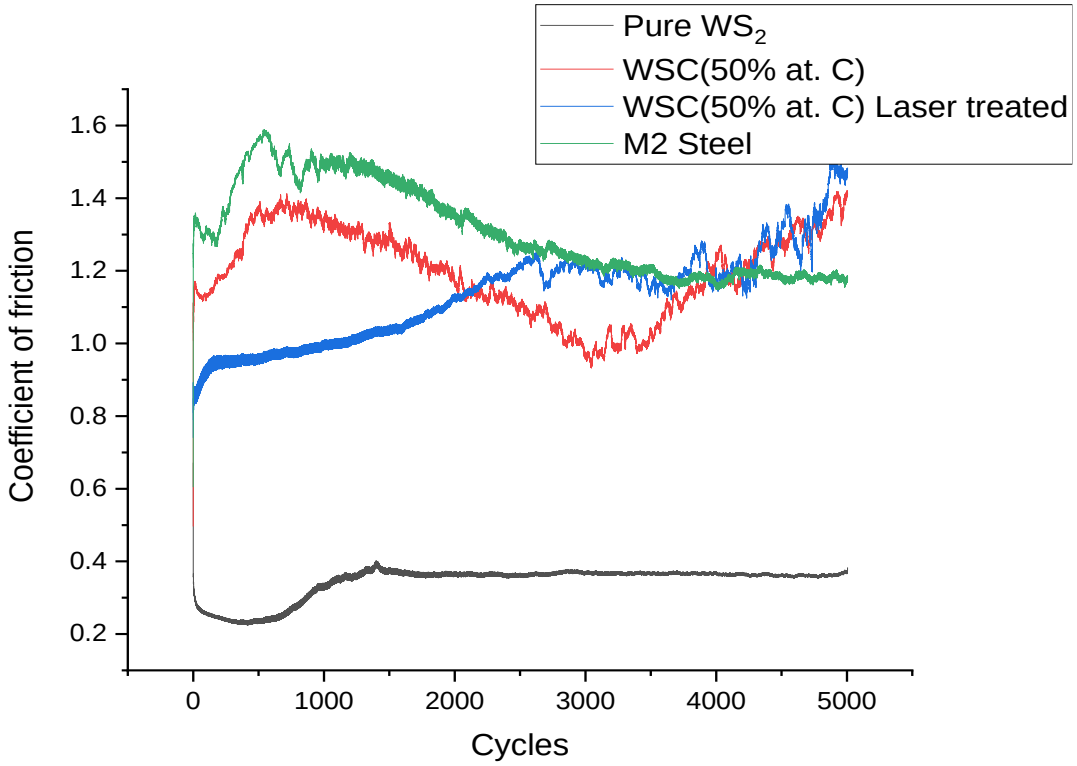

Figure 16 Coefficient of friction at room temperature

Interestingly laser-treated WSC coating showed significantly lesser COF as compared to untreated WSC coating. To understand the reason, 3 D profilometry on the laser-treated sample was done. It was found that inside wear tracks, the laser-treated areas appeared to have pits, which means during sliding, the laser-treated areas are removed due to their softer nature. This can be beneficial as this material can act as a lubricant and, indeed, the laser-treated sample showed lower COF compared to the as deposited sample. Nevertheless, it seems that this removed material is consumed during sliding and, afterwards, friction increases (see Figure 17 and Figure 18).

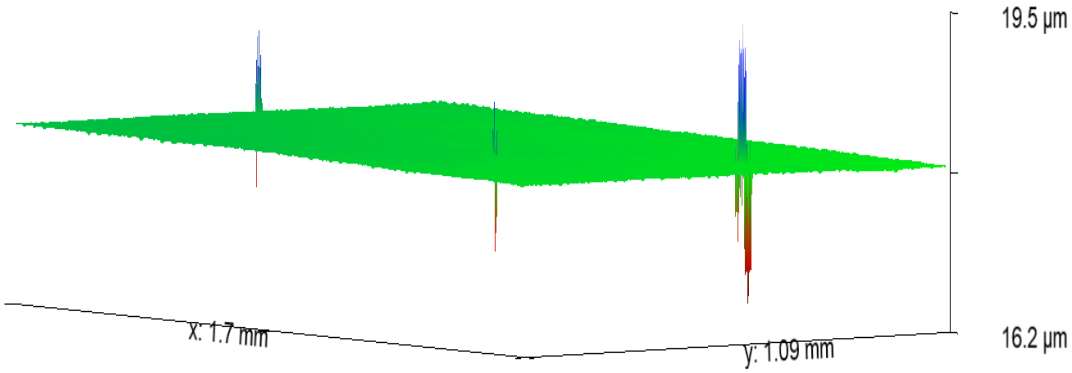

Figure 17 3D view of pits inside wear scar for laser treated WSC50

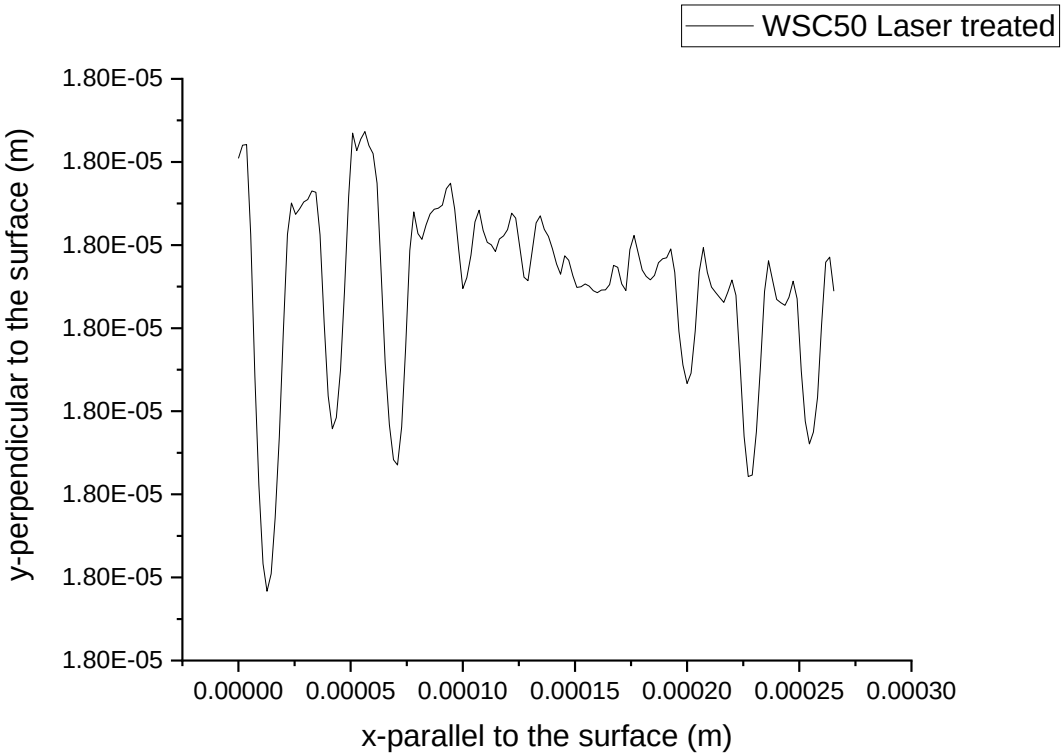

Figure 18 Line profile for pits inside wear scar in laser-treated WSC50

4.4.2. Wear analysis

Wear tracks were analyzed for pure WS_2 coating with a 3 D profilometer, and wear volume was calculated. There was no wear found in the case of treated and untreated WSC, and wear was calculated only for WS_2 coating. The four different locations chosen to scan were from the circumference of the wear scar. The cross-sectional area was calculated and multiplied by the circumference to get the wear volume. To find the specific wear rate, wear volume was divided by load and total sliding distance. Specific wear rate was calculated to be $3.6 \times 10^{-5} \frac{mm^3}{N.m}$.

EDS analysis was conducted inside the wear track for the WS_2 coating. Figure 19 shows the SEM image of the wear track at four different locations. At point 2.3, there was the presence of C and N, which is possibly because of the transfer of NBR rubber on the surface.

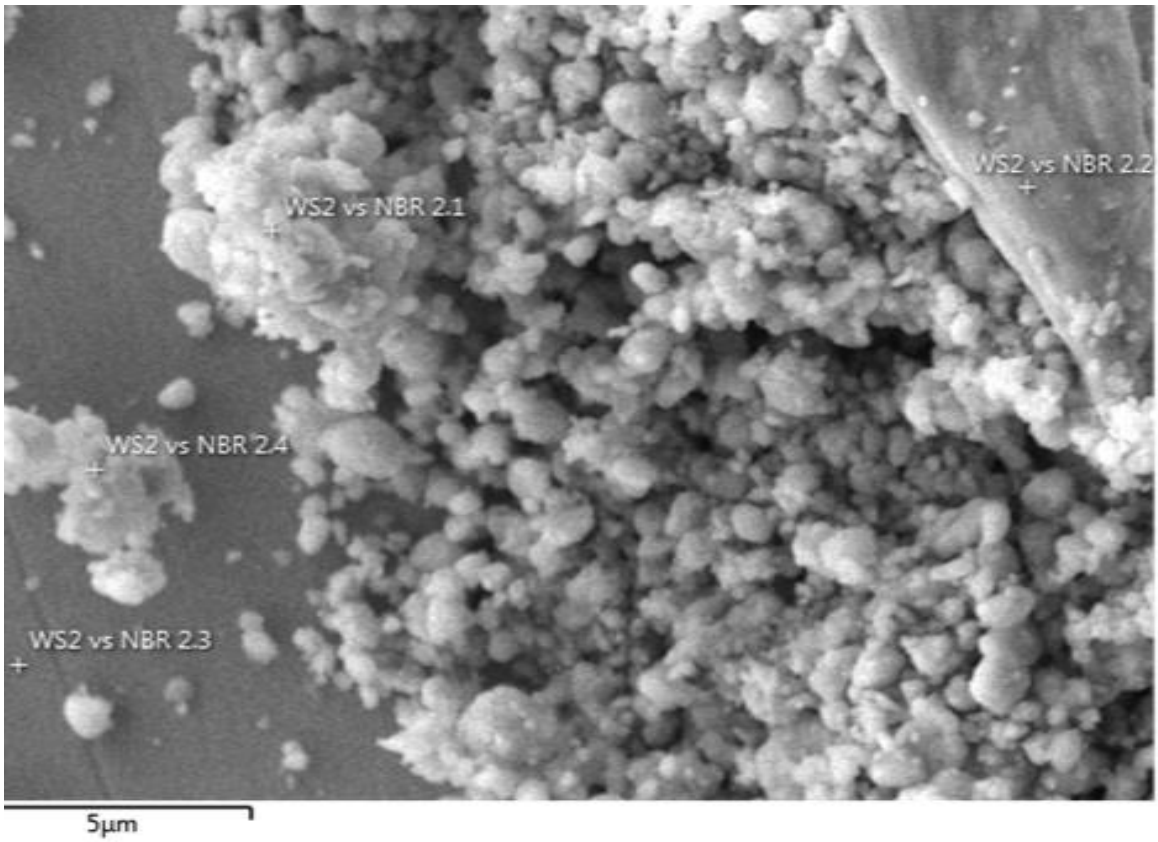

Figure 19 SEM image of inside of wear track for WS_2

There is also oxide formation inside the wear track which might be an indication of the formation of WO_3. In one of the locations, a significant amount of Cr was also found which can be due to wear off coating that resulted in EDS detecting the Cr from the substrate.

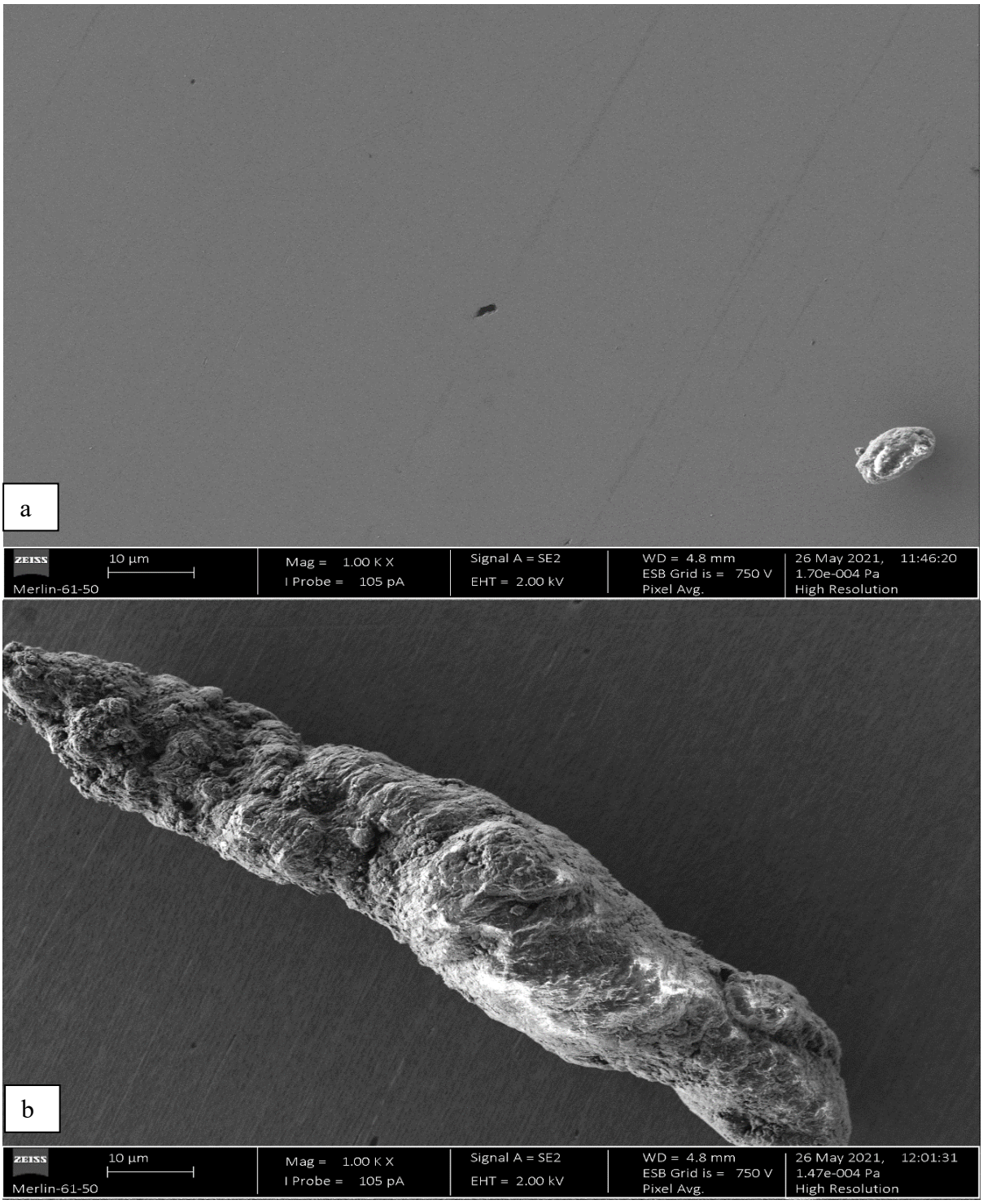

Figure 20 SEM images for uncoated steel a) Inside scar b) NBR rubber

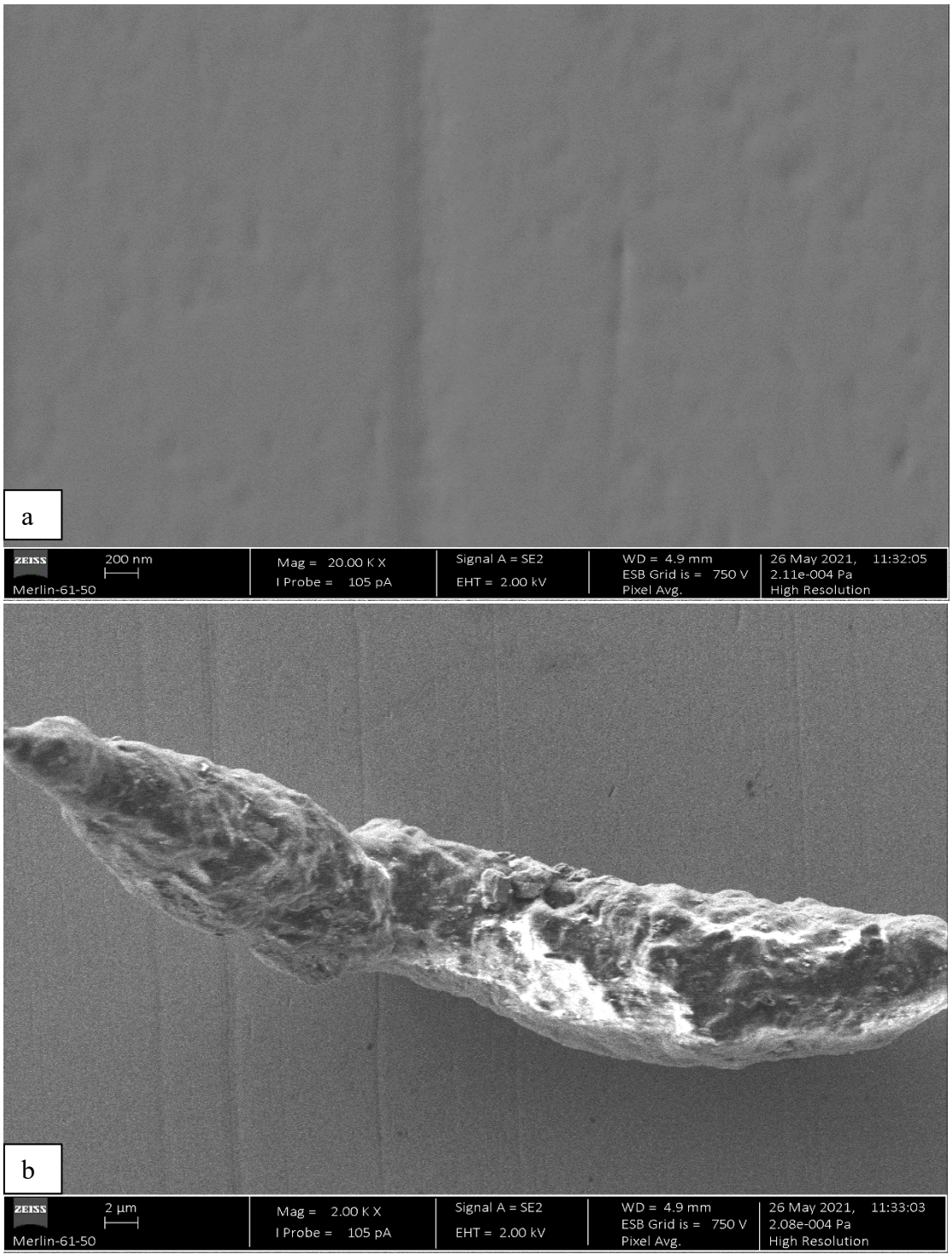

Figure 21 SEM images for WSC a) Inside scar b) NBR rubber

Figure 20a, 21a, and 22a to shows that there was no significant wear observed in case of both WSC and steel samples. The only thing that can be observed is smoothening of the surface and minor abrasive marks. Figure 20b and 21b shows the SEM image of asperities observed inside the wear track which can be due to the wearing off of the NBR ball during the test.

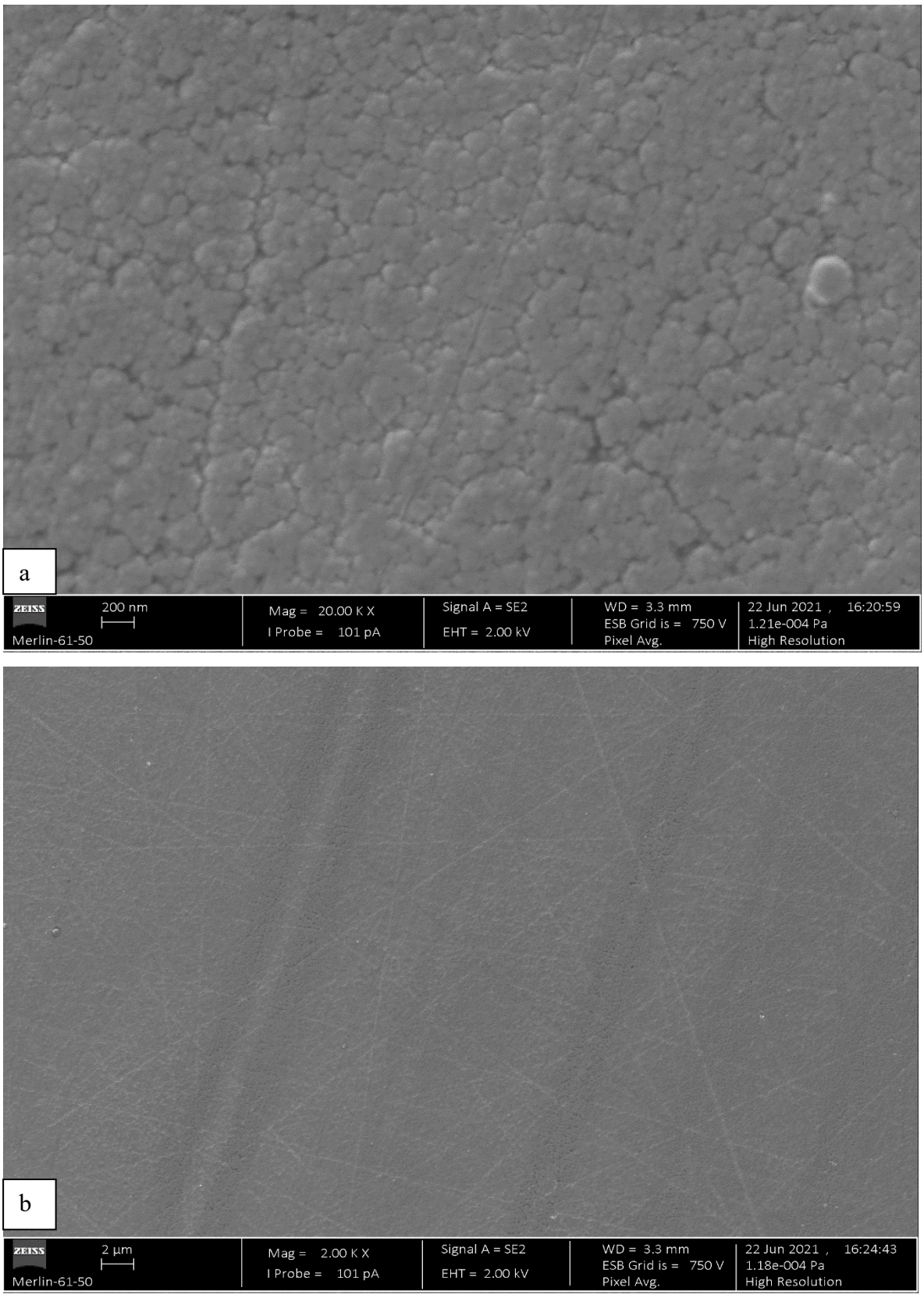

Figure 22 SEM images for WSC laser treated coating a) 20k magnification b) 2k magnification

5. CONCLUSION

The work presented in this thesis is focused on the effect of laser treatment on the tribological behaviour of C-alloyed WS_2 coating in rubber contact. Thin films of WS_2 and WSC were deposited by magnetron sputtering. Four different samples were prepared which are uncoated M2 steel, WS_2, untreated, and UV laser-treated WSC (50 at. % C).

SEM images showed improved porosity and compactness in the coating as a result of C-alloying. Raman spectroscopy presented the typical crystalline peaks for the unalloyed WS_2 coating while for the W-S-C coating it revealed the amorphous nature of the carbon phase. For the laser treated sample it revealed crystallization of WS2 in the treated areas, with signs of graphitization for the areas that are slightly overexposed. XRD diffractogram showed broad amorphous carbon peak in the region, $2\theta \approx 30° - 50°$, and showed no structural difference in WSC coating when treated by laser as XRD technique is not suitable to detect small-sized WS_2 crystals.

Alloying of C in WS_2 coatings resulted in an increase in hardness from ~0.23 GPa to ~7 GPa. The hardness of the WSC coating in treated zones was reduced to ~3 GPa from ~7 GPa.

The intended mechanism of low friction for pure and alloyed WS_2-based coatings is the formation of WS_2 tribofilms on the outermost surface. The reason for easy shearing and ease of sliding along the sliding direction is the horizontal alignment of WS_2 tribofilms. Thus, having crystalline and horizontally aligned WS_2 in the coating are necessary conditions. Pure WS_2 coatings have standing platelets and the basal planes realign in the direction of sliding, while for secondary coatings (amorphous or poorly crystalline), there is a rearrangement of the planes in the contact. However, WS_2 tribofilms formation is true in both cases by reorientation of the basal planes during the running-in period in order to realign them in the direction of sliding.

In conclusion, laser treatment of the coatings mainly influenced the running-in and the early steady-state tribological behaviour of the coatings.

6. REFERENCES

[1] K. Holmberg, P. Kivikytö-Reponen, P. Härkisaari, K. Valtonen e A. Erdemir, "Global energy consumption due to friction and wear in the mining industry," *Tribology International,* vol. 115, pp. 116-139, 2017.

[2] H. P. Jost, "Lubrication (tribology) education and research." Jost Report"," Department of Education and Science, HMSO. Reino Unido, 1966.

[3] T. Polcar, M. Evaristo e A. Cavaleiro, "Comparative study of the tribological behavior of self-lubricating W–S–C and Mo–Se–C sputtered coatings," *Elsevier,* vol. 266, nº 3-4, pp. 388-392, 2009.

[4] D. Packham, Mould sticking, fouling and cleaning, vol. 13, 2002.

[5] "Mould releases – an overview, Reinforced Plastics," vol. 52, nº 7, pp. 32-34, 2008.

[6] BryCoat, "BryCoat Tungsten Disulfide (WS2)," 2015. [Online]. Available: https://www.brycoat.com/surface-engineering/got-friction-brycoat-dry-film-lubricant-coatings/got-friction-brycoat-tungsten-disulfide-ws2-dry-lubricant-coatings/. [Acedido em 10 January 2020].

[7] C. Enrico, "Tribology and Industry: From the Origins to 4.0," *Frontiers in Mechanical Engineering ,* vol. 5, nº 2297-3079 , p. 55, 2019.

[8] S. Affatato e L. Grillini, "Topography in bio-tribocorrosion," *Woodhead Publishing,* pp. 1-22a, 2013.

[9] P. Anton, "Basics of tribology," Anton Paar, 2015. [Online]. Available: https://wiki.anton-paar.com/br-pt/basics-of-tribology/. [Acedido em 10 1 2021].

[10] B. Bhushan, "Wear Mechanisms," em *Tribology and Mechanics of Magnetic Storage Devices,* NY, Springer, 1996, pp. 412-546.

[11] N. Corporotion, “Common Causes of Machine Failures,” Machinery Lubrication, [Online]. Available: https://www.machinerylubrication.com/Read/29331/machine-failure-causes. [Acedido em 12 01 2021].

[12] Y. Yan, “Tribology and tribocorrosion testing and analysis of metallic biomaterials,” *Woodhead Publishing,* vol. 2, nº ISBN 9780081026663, pp. 213-234, 2019.

[13] T. W. Scharf e S. V. Prasad, “Solid lubricants: a review,” *Journal of Materials Science,* vol. 48, p. 511–531, 2013.

[14] C. Wikipedia, “Transition metal dichalcogenide monolayers,” 2020. [Online]. Available: https://en.wikipedia.org/w/index.php?title=Transition_metal_dichalcogenide_monolayers&oldid=993527448. [Acedido em 10 1 2021].

[15] A. Devadoss, N. Srinivasan, V. Devarajan, A. N. Grace e S. Pitchaimuthu, “Electrocatalytic properties of two-dimensional transition metal dichalcogenides and their hetrostructures in energy applications,” *Elsevier,* pp. 215-241, 2020.

[16] “T. Polcar, Self-lubricating nanostructured coatings based on transition metal dichalcogenides alloyed with carbon. Habilitation thesis, Czech Technical University in Prague, 2009.”.

[17] A. Voevodin, J. O'Neill e J. Zabinski, “Nanocomposite tribological coatings for aerospace applications,” *Surface and Coatings Technology,* vol. 116–119, pp. 36-45., 1999.

[18] J. M. Martin, C. Donnet, T. L. Mogne e T. Epicier, “Superlubricity of molybdenum disulphide,” *Phys. Rev. B,* vol. 48, nº 14, pp. 10583-10586, 1993.

[19] T. Vuchkov, T. B. Yaqub, M. Evaristo e Albano Cavaleiro, “Synthesis, microstructural and mechanical properties of self-lubricating Mo-Se-C coatings deposited by closed-field unbalanced magnetron sputtering,,” *Surface and Coatings Technology,* vol. 394, p. 125889, 2020.

[20] C. Dong, C. Yuan, X. Bai, X. Yan e Z. Peng, “Tribological properties of aged nitrile butadiene rubber under dry sliding conditions,,” Vols. %1 de %2222-223, nº 0043-1648, pp. 226-237, 2015.

[21] B. Jiang, X. Jia, Z. Wang e Tao Wang, “Influence of Thermal Aging in Oil on the Friction and Wear Properties of Nitrile Butadiene Rubber,” *Tribol lett,* vol. 86, p. 67, 2019.

[22] M.-x. Shen, B. Li, S. Li, G.-y. Xiong, D.-h. Ji e Z.-n. Zhang, “Effect of particle concentration on the tribological properties of NBR sealing pairs under contaminated water lubrication conditions,,” *Science direct,* Vols. %1 de %2556-557, nº 0043-1648, 2020.

[23] J. Yang, M. Tian, Q.-X. Jia, L. Zhang e X. Li, “Influence of graphite particle size and shape on the properties of NBR,” *Journal of applied polymer science,* Vols. %1 de %24007-4015, p. 102, 2006.

[24] M. Evaristo, T. Polcar e A. Cavaleiro, “Tribological behaviour of C-alloyed transition metal dichalcogenides (TMD) coatings in different environments,” *Int J Mech Mater Des,* vol. 4, pp. 137-143, 2008.

[25] H. Hadouda, J. Bernède, J. Pouzet e R. L. Ny, “Physicochemical characterization of MoS2 films obtained by solid state reaction between the constituents of a multilayer Mo/S…/Mo/S structure,” *Materials Science and Engineering: B,* vol. 45, nº 1-3, pp. 9-16, 1997.

[26] *E. Bermann, G. Melet, C. Muller, A. Simon-Vermot, Tribol. Int. 14 (1981) 329.*

[27] N. Renevier, J. Hamphire, V. Fox, J. Witts, T. Allen e D. Teer, “Advantages of using self-lubricating, hard, wear-resistant MoS2-based coatings,” *Surface and Coatings Technology*, vol. 142–144, nº 0257-8972, pp. 67-77, 2001.

[28] T. B. Yaqub, S. Bruyere, J.-F. Pierson, T. Vuchkov e A. Cavaleiro, “Insights into the wear track evolution with sliding cycles of carbon-alloyed transition metal

dichalcogenide coatings," *Surface and Coatings Technology,* vol. 403, nº 126360, p. 126360, 2020.

[29] A. Jagminas, G. Niaura e R. Žalnėravičius, "Laser Light Induced Transformation of Molybdenum Disulphide-Based Nanoplatelet Arrays.," *Scientific Reports,* vol. 6, p. 37514, 2016.

[30] M. p. contributors, "What are Properties of Molybdenum High-speed Steel – AISI M2 – Definition," [Online]. Available: https://material-properties.org/what-are-properties-of-molybdenum-high-speed-steel-aisi-m2-definition/. [Acedido em 17 01 2021].

[31] D. M. Mattox, "Introduction," em *Handbook of physical vapor deposition (PVD) processing*, William Andrew Publishing, 2010, pp. 1-24.

[32] S. Swann, "Magnetron sputtering," em *Physics in technology*, IOP publishing ltd., 1988, pp. 67-75.

[33] M. Evaristo, A. Nossa e A. Cavaleiro, "W–S–C sputtered films: Influence of the carbon alloying method on the mechanical properties," *Surf. Coatings Technol.,* vol. 200, nº 1-4, p. 1076–1079., 2005.

[34] A. Tiwari, J. Rawlins e L. H. Hihara, "Intelligent Coatings for Corrosion Control," *Butterworth-Heinemann,* vol. 1, pp. 1-746, 2014.

[35] T. Afaneh, P. K. Sahoo, I. A. P. Nobrega, Y. Xin e H. R. Gutiérrez, "Laser-Assisted Chemical Modification of Monolayer Transition Metal Dichalcogenides," *Adv. Funct. Mater.,* vol. 28, 2018.

[36] "W. Steen and J. Mazumder, Laser Material Processing. London: Springer, 2010.".

[37] "M. E. McConney, "Direct synthesis of ultra-thin large area transition metal dichalcogenides and their heterostructures on stretchable polymer surfaces," J. Mater. Res., vol. 31, no. 7, pp. 967–974, 2016.".

[38] M. Shamshiri, A. Manaia, T. Vuchkov, A. Carvalho, G. Gaspar, A. Fernandes, S. Heydarian, D. F. Costa e A. Cavaleiro, "Influence of laser structural patterning on the tribological performance of C-alloyed W-S coatings," *Surf. Coat. Technol.,* vol. 394, p. 125822, 2020.

[39] J. W. Kang, "Effect of laser power and scanning speed on the microstructure and mechanical properties of SLM fabricated Inconel 718 specimens," *Mater. Sci. Eng. Int. J.,* vol. 3, nº 3, 2019.

[40] C. Hitz, C. Breck, J. J. wing e J. Heht, "Introduction to Laser Technology,," *John Wiley & Sons,,* vol. 4, pp. 1-312, 2012.

[41] D. Henry, "Electron-Sample Interactions," Louisiana State University, 10 11 2016. [Online]. Available: https://serc.carleton.edu/research_education/geochemsheets/electroninteractions.html. [Acedido em 16 01 2021].

[42] H. Garbacz e A. Królikowski, "Corrosion resistance of nanocrystalline titanium," *Elsevier,* pp. 145-173, 2019.

[43] G. W. Stachowiak e A. W. Batchelor, "Characterization of Test Specimens," *Elsevier,* vol. 44, pp. 115-150, 2004.

[44] R. Wolthuis, T. B. Schut, P. Caspers, H. Buschman, T. Romer, H. Bruining e G. Puppels, "Raman Spectroscopic Methods for In Vitro and In Vivo Tissue Characterization," *Academic Press,* vol. 32, pp. 433-455, 1999.

[45] B. L. Dutrow e C. M. Clark, "X-Ray Powder diffaraction ()XRD," SERC, 14 02 2020. [Online]. Available: https://serc.carleton.edu/research_education/geochemsheets/techniques/XRD.html. [Acedido em 16 01 2021].

[46] M. V. Maria Kaliva, "Nanomaterials Characterization," *Polymer Science and Nanotechnology, Elsevier,* pp. 401-433, 2020.

[47] S. Baker e J. Liu, “Nanoindentation Techniques,” *Elsevier,* 2016.

[48] M. M. Maru e D. K. Tanaka, “Influence of loading, contamination and additive on the wear of a metallic pair under rotating and reciprocating lubricated sliding,” *Journal of the Brazilian Society of Mechanical Sciences and Engineering,* vol. 28, nº 3, pp. 278-285, 2006.

[49] “Regula, M., Ballif, C., Moser, J. H., and Lévy, F., 1996, “Structural, chemical, and electrical characterisation of reactively sputtered WSx thin films,” Thin Solid Films, 280(1-2), pp. 67–75.”.

[50] J. R. A. C. Ferrari, “Interpretation of Raman spectra of disordered and amorphous carbon.,” *Physical Review B,* vol. 20, p. 61, 2000.

[51] G. Raju, “Tribological study of TMD coatings for rubber applications,” 2015.

[52] J. Green, “An Overview of Magnetron Sputtering,” 30 01 2021. [Online]. Available: https://www.sputtertargets.net/blog/an-overview-of-magnetron-sputtering.html.